Technical University of Lodz
FACULTY OF MECHANICAL ENGINEERING
DIVISION OF DYNAMICS

Krzysztof Jankowski
137876

MASTER OF SCIENCE THESIS
Mechanical Engineering and Applied Computer Science

Dynamics of double pendulum with parametric vertical excitation

supervision:
prof. dr hab. inż. Tomasz Kapitaniak

Lodz, 11.07.2011

INNOVATIVE ECONOMY
NATIONAL COHESION STRATEGY
FNP
Foundation for Polish Science
EUROPEAN UNION
EUROPEAN REGIONAL DEVELOPMENT FUND

Technical University of Lodz
Faculty of Mechanical Engineering
Division of Dynamics
International Faculty of Engineering

Lodz, 2011

CONTENTS

Preface

This master of science thesis is a part of "Project TEAM of Foundation for Polish Science" realising the investigation and analysis of the project "Synchronization of Mechanical Systems Coupled through Elastic Structure". It is supported by "Innovative Economy: National Cohesion Strategy". The programme is financed by "Foundation for Polish Science" from the European funds as the plan of "European Regional Development Fund". The project is mainly focused on the following issues:

- *Identification of possible synchronous responses of coupled oscillators, and existence of synchronous clusters as well*
- *Dynamical analysis of identical coupled systems suspended on elastic structure in context of the energy transfer between systems*
- *Investigation of phase or frequency synchronization effects in groups of coupled non-identical systems*
- *Developing methods of motion stability control of considered systems*
- *Investigation of time delay effects in analyzed systems.*
- *Developing the idea of energy extraction from ocean waves using a series of rotating pendulums.*

INNOVATIVE ECONOMY
NATIONAL COHESION STRATEGY
FNP Foundation for Polish Science
EUROPEAN UNION
EUROPEAN REGIONAL DEVELOPMENT FUND

1. Introduction

The pendulum is a very well-known object. It recalls the construction of the old-fashioned mechanical clocks, which even in times of quartz timepieces, digital and atomic ones remain relatively common. The pendulum`s attraction and interest is associated with the familiar regularity of its swings, and as the consequence its bond to the fundamental natural force of gravity.

The pendulum might be spotted in variety of different areas, starting from the most obvious mechanics, through the usage of metronome by music schools, ending on the film by Umberto Eco Foucault`s Pendulum.

The history of the pendulum might be begin with a recall of the tale of Galileo`s observation of the swinging chandeliers in the cathedral in Pisa. “By using his own heart rate as a clock, Galileo presumably made the quantitative observation that, for a given pendulum, the time period of a swing was independent of the amplitude of the pendulum`s displacement. Like many other seminal observations in science, this one was only an approximation of reality. Yet, it had the main ingredients of the scientific enterprise; observation, analysis and conclusion. Galileo was one of the first of the modern scientists, and the pendulum was among the first objects of scientific enquiry” [1].

There is a wide range of pendulums. The very first and the most common is a simple pendulum, characterised by the small amplitude. Neglecting the energy loss factors, there is no need for energizing this device through the forcing mechanisms. Taking a relatively small swing of the pendulum, makes it possible to linearize the equations and thus formulate the solution of the motion of this device. By adding another simple pendulum to the end of the first one, we obtain more complex system (series connection of the pendulums). Further introduction of complicating factors like elastic joint, energy losses and finally subjected the whole system to the periodic oscillation might lead to the chaotic motion, what is the subject of this paper.

1.1 The examined system

This master of science thesis is to investigate the tendencies and behaviour of the double pendulum subjected to the parametric, vertical excitation. The system of investigation is presented in the figure 1.

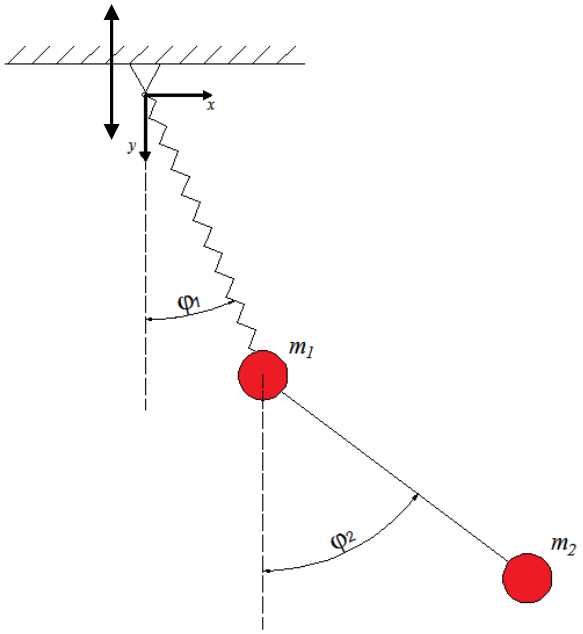

Fig. 1 Double pendulum system.

The examined system consists of 2 concentrated masses attached to the ends of the joints. The joints are assumed to be massless, the first one is elastic, whereas the second one has the fixed length.

1.2 Aim of the thesis

The aim of this paper is to numerically investigate and analyse the system of double pendulum with parametric, vertical excitation, presented in chapter 7.2. The research include influence of the selected control parameters on the behaviour of the double pendulum system as well as the bifurcation analysis carried for different control parameters. Additionally, the research includes presentation of the behaviour of the system using Poincaré maps, phase portraits and time diagrams.

2. Basic concepts of physics and mathematics

In this chapter basic definitions and theorems, used in the further part of this paper, are introduced. They are put in order of appearance and complexity. There are subchapters devoted to physical and mathematical section.

2.1 Concepts of physics

Generalised coordinates (definition 1, [6])

Generalised coordinates is the set of independent coordinates explicitly defining position of the system, number of generalised coordinates is equal to the number of degrees of freedom of the system.

Ties (definition 2, [6])

The factors resulting in limitation of the motion of the material points are called ties. The limitation of the freedom of movement of the system consisting of n material points can be analytically expressed by means of equations and inequalities presented below:

$$f_k = (\vec{r}_1, \vec{r}_2, \dots, \vec{r}_\mathrm{n}, t) = 0 \qquad \text{for} \qquad k = (1, 2, \dots, p), \tag{2.1}$$

or

$$\varphi_1 = (\vec{r}_1, \vec{r}_2, \dots, \vec{r}_\mathrm{n}, t) \leq 0 \qquad \text{for} \qquad l = (1, 2, \dots, \varphi), \tag{2.2}$$

are called equations of ties.

Mobility of the system (definition 3, [6],[8])

By the mobility of the system we specify its number of degrees of freedom. This might be understood as a number of independent input motions, either translational or rotational ones, defining the orientation of the body or system. There is a relation between an arbitrary point of the system and the remaining ones. Namely, there are n – 1 distances between the points. Then, subsequently free rigid body has the number of degrees of freedom, given by the equation:

$$f = 3n - \frac{n(n-1)}{2}. \tag{2.3}$$

Kinetic energy (definition 4, [6])

The quantity given by (2.4) is called the kinetic energy of the material point.

$$T = \frac{m\vec{v}^2}{2}. \tag{2.4}$$

Total kinetic energy (definition 5, [6])

The quantity given by (2.5) is called the total kinetic energy of the material point.

$$T = \sum_{i=1}^{n} \frac{m_i \vec{v}_i^2}{2}. \tag{2.5}$$

Potential energy (definition 6, [4],[6])

If there exists function $V(\vec{r}, t)$ such that :

$$\vec{V} = -gradV = -\left(\vec{\imath}\,\frac{\partial V}{\partial x} + \vec{\jmath}\,\frac{\partial V}{\partial y} + \vec{k}\,\frac{\partial V}{\partial k}\right), \tag{2.6}$$

then it is said, that force $\vec{F}$ is potential and function $V(\vec{r}, t)$ is called the potential of that force. We see that, the potential force is only dependent on the position and time $\vec{F}(\vec{r}, t)$. If the potential is not dependent on the time - $V(\vec{r})$, then it is said, that

the force $\vec{F}$ is conservative and then $V(\vec{r})$ is called the potential energy of the material point in position $\vec{r}$ in the field of force $\vec{F}(\vec{r})$.

Considering distances significantly smaller than radius of the earth, then one can assume, that gravitational field is uniform, of vertical direction and backward sense. The potential energy of mass m, placed over distance h, with respect to preselected frame of reference is equal to the product of mass m, gravitational acceleration g and that distance h:

$$V = mgh. \tag{2.7}$$

Taking into consideration an elastic element obeys the Hook`s law, there is the proportionality of the acting force to its elongation. Hence, when the length of the (for instance) spring is given by $a + x$, then the force in spring is as follows:

$$F = k\,x\,\boldsymbol{i}, \tag{2.8}$$

where i is a versor.

The constant k is called the stiffness of the elastic element. The force F is positive, when x is positive and negative. In case of x being negative, it shows the tendency of the spring to return to the unconstrained length, regardless the fact whether it was stretched or compressed.

The work done by the force acting on the elastic element, while its length is changed from a to $a + x$, is given by:

$$\int_0^x -\boldsymbol{k\xi i}\,\boldsymbol{d\xi i} = -\frac{kx^2}{2}. \tag{2.9}$$

The above expression shows, that force in the elastic element is a conservative force of the following potential energy:

$$V = \frac{kx^2}{2}. \tag{2.10}$$

Conservation of energy (definition 7, [4])

In conservative systems, sum of kinetic and potential energy is constant.

$$T + V = const. \tag{2.11}$$

2.2 Concepts of mathematics

Ordinary differential equations (definition 8, [5])

Ordinary differential equation (ODE) is the equation including an independent variable x, unknown function y and its derivatives $y', y'', \dots, y^{(n)}$.

$$F\left(x, y, y', \dots, y^{(n)}\right) = 0, \tag{2.12}$$

where F: $R^{n+2} \rightarrow R$.

The solution of the equation given by (2.20) in $[a, b]$ is the function of the following properties:

$$\bigwedge_{x \in [a,b]} F\left(x, y(x), y'(x), \dots, y^{(n)}(x)\right) = 0. \tag{2.13}$$

Lagrange`s equations of the second kind (definition 9, [4])

Let us consider the system of N degrees of freedom, described by N generalised coordinates q_i, $i = 1, 2, \dots, n$. The Lagrange`s equations of the second kind are formulated as follows:

$$\frac{d}{dt}\left(\frac{\partial T}{\partial \dot{q}_i}\right) - \frac{\partial T}{\partial q_i} + \frac{\partial D}{\partial \dot{q}_i} + \frac{\partial V}{\partial q_i} = Q_i, \tag{2.14}$$

where T is the kinetic energy and V is potential energy of the system. The function D is the Rayleigh dissipation function, whereas Q_i is the generalised external force applied to the system. The value of Q_i can be expressed as follows:

$$Q_i = \sum_l F_l \frac{\partial r_l}{\partial q_i} + \sum_l M_l \frac{\partial \omega_l}{\partial \dot{q}_i}, \tag{2.15}$$

where F_l and M_l are external force and external moment vectors respectively. The index l indicates, which of the forces (or moments) are considered, r_l is the position vector with respect to the point of application of the force F_l; $\omega_l$is the angular velocity of the system with respect to the application point of the moment M_l. Products presented in the equation (2.15) are scalar values.

3. Simple pendulum

According to [1], simple pendulum can be treated as the perfect model of a real pendulum. It is build with a concentrated mass m, attached to a rod with negligible mass and of initial length l. Whole system is fastened to a frictionless pivot point, as shown in fig. 2.

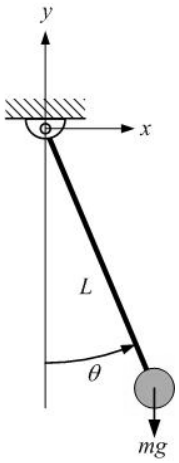

Fig. 2 Simple pendulum.

If the pendulum is displaced from its equilibrium position and released, i.e. potential energy is turned into kinetic, it will oscillate around equilibrium position with a constant amplitude for infinitely long time – the pendulum will be subjected to the harmonic motion. As mentioned, the frictionless pivot point is assumed and no air resistance to motion. According to the Newton`s second law, force is equal to mass and acceleration product, given by the equation:

$$ml\frac{d^2\theta}{dt^2} = -mg\,sin\theta, \tag{3.1}$$

where θ is the angular displacement of the pendulum from the equilibrium position and g is the gravitational acceleration. Considering very small amplitude of oscillation, $sin\,\theta \approx \theta$, after simplification we obtain:

$$\frac{d^2\theta}{dt^2} + \frac{g}{l}\theta = 0. \tag{3.2}$$

Solving the above equation for θ, we receive:

$$\theta = \theta_0 \, sin(\omega t + \phi_0), \tag{3.3}$$

where θ_0 is the angular amplitude of the swing and ϕ_0 is the initial phase.

$$\omega = \sqrt{\frac{g}{l}}, \tag{3.4}$$

ω is the angular frequency of the pendulum, and its period T is given by the following formula (linearized approximation):

$$T = 2\pi \sqrt{\frac{l}{g}}, \tag{3.5}$$

It should be pointed that for a given pendulum its period is constant and is only dependent on its length.

Taking angular displacement θ and its derivative – angular velocity $\dot{\theta}$, respectively, as the functions of time we receive:

$$\theta = \theta_0 \sin(\omega t + \phi_0), \tag{3.6}$$

$$\dot{\theta} = \theta_0 \omega \cos(\omega t + \phi_0), \tag{3.7}$$

and now it is possible to create graph depicting their dependencies – time series.

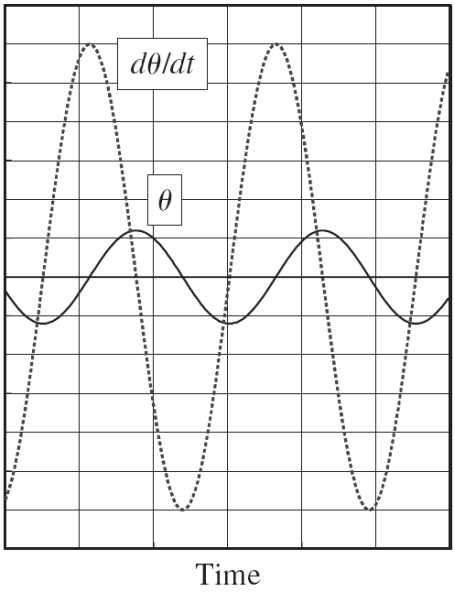

Fig. 3 Time series for angular displacement and angular velocity [1].

As shown in figure 3, the displacement and velocity are out of phase by 90 degrees, it means that, if one quantity reaches its maximum, the other one has value of zero – when pendulum has maximum velocity, its displacement is equal to zero and vice versa.

4. Double pendulum

Basing on [1], let us consider the system presented in figure 4:

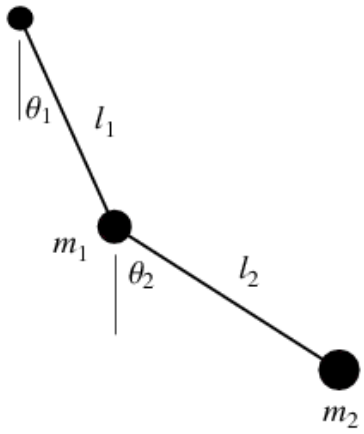

Fig. 4 Double pendulum.

It consist of two simple pendulums connected in series in such a manner that the second pendulum is attached to the bob of the first one [7]. While we are dealing with two angular degrees of freedom, denoted as θ_1 and θ_2, the behaviour of the system will more complicated than in case of the simple pendulum. Due to the occurrence of the additional degree of freedom, as well as more complex motion, the system is prone to chaotic motion and very sensitive to initial conditions [1].

The potential energy of the double pendulum is calculated as the reference of the lifted pendulum to the zero potential energy state at equilibrium position, thus the equation takes the following form:

$$V = m_1 g l_1 (1 - cos\theta_1) + m_2 g [l_1 (1 - cos\theta_1) + l_2 (1 - cos\theta_2)]. \tag{4.1}$$

In order to formulate kinetic energy equation will make use of derivation of x and y coordinates of the system, which are presented below:

$$x_2 = l_1 sin\theta_1 + l_2 sin\theta_2,$$

$$y_2 = -l_1 cos\theta_1 - l_2 cos\theta_2. \tag{4.2}$$

After derivation and summing up the expressions, we are able to specify the final form of the kinetic energy:

$$K = \frac{1}{2}m_1 l_1^2 \dot{\theta}_1^2 + \frac{1}{2}m_2 l_1^2 \dot{\theta}_1^2 + \frac{1}{2}m_2 l_2^2 \dot{\theta}_2^2 + m_2 l_1 l_2 \cos(\theta_1 - \theta_2)\, \dot{\theta}_1 \dot{\theta}_2. \tag{4.3}$$

The simplest Lagrangian equation is as follows:

$$\frac{d}{dt}\left(\frac{\partial L}{d\dot{\theta}_i}\right) - \left(\frac{\partial L}{d\theta_i}\right) = 0. \tag{4.4}$$

Using the Lagrange`s equations and making adequate substitutions we may formulate coupled equations of motion for the system given:

$$\ddot{\theta}_1 = -\frac{l_2}{\mu l_1}\ddot{\theta}_2 \cos(\theta_1 - \theta_2) - \frac{l_2}{\mu l_1}\dot{\theta}_2^2 \sin(\theta_1 - \theta_2) - \frac{g}{l_1} sin\theta_1, \tag{4.5}$$

$$\ddot{\theta}_2 = -\frac{l_1}{l_2}\ddot{\theta}_1 \cos(\theta_1 - \theta_2) + \frac{l_1}{l_2}\dot{\theta}_1^2 \sin(\theta_1 - \theta_2) - \frac{g}{l_2} sin\theta_2, \tag{4.6}$$

where:
$\mu = 1 + (m_1 + m_2)$.

To decompose angular acceleration terms we substitute them by placing the second equation in the first one and vice-versa, we receive:

$$\ddot{\theta}_1 = \frac{g(\sin\theta_2 \cos(\theta_1 - \theta_2) - \mu \sin\theta_1) - \left(l_2\dot{\theta}_2^2 + l_1\dot{\theta}_1^2 \cos(\theta_1 - \theta_2)\right)\sin(\theta_1 - \theta_2)}{l_1(\mu - \cos^2(\theta_1 - \theta_2))}, \tag{4.7}$$

$$\ddot{\theta}_2 = \frac{g\mu(\sin\theta_1 \cos(\theta_1 - \theta_2) - \sin\theta_2) + \left(\mu l_1\dot{\theta}_1^2 + l_2\dot{\theta}_2^2 \cos(\theta_1 - \theta_2)\right)\sin(\theta_1 - \theta_2)}{l_2(\mu - \cos^2(\theta_1 - \theta_2))}. \tag{4.8}$$

Introducing new variables, ω_1 and ω_2, allows us to formulate four equations, making it possible to facilitate numerical solution.

$$\dot{\theta}_1 = \omega_1, \tag{4.11}$$

$$\dot{\omega}_1 = \frac{g(\sin\theta_2 \cos(\theta_1 - \theta_2) - \mu \sin\theta_1) - (l_2\omega_2^2 + l_1\omega_1^2 \cos(\theta_1 - \theta_2)) \sin(\theta_1 - \theta_2)}{l_1(\mu - \cos^2(\theta_1 - \theta_2))}, \tag{4.9}$$

$$\dot{\theta}_2 = \omega_2, \tag{4.12}$$

$$\dot{\omega}_2 = \frac{g\mu(\sin\theta_1 \cos(\theta_1 - \theta_2) - \sin\theta_2) + (\mu l_1\omega_1^2 + l_2\omega_2^2 \cos(\theta_1 - \theta_2)) \sin(\theta_1 - \theta_2)}{l_2(\mu - \cos^2(\theta_1 - \theta_2))}. \tag{4.10}$$

To obtain, chaotic behaviour, according to the [1], we introduce mass $m_2 < m_1$ and exemplary initial values of angular displacements and angular velocities $\theta_1 = 0.5$; $\theta_2 = 2.0$; $\omega_1 = 0$; $\omega_2 = 0$.

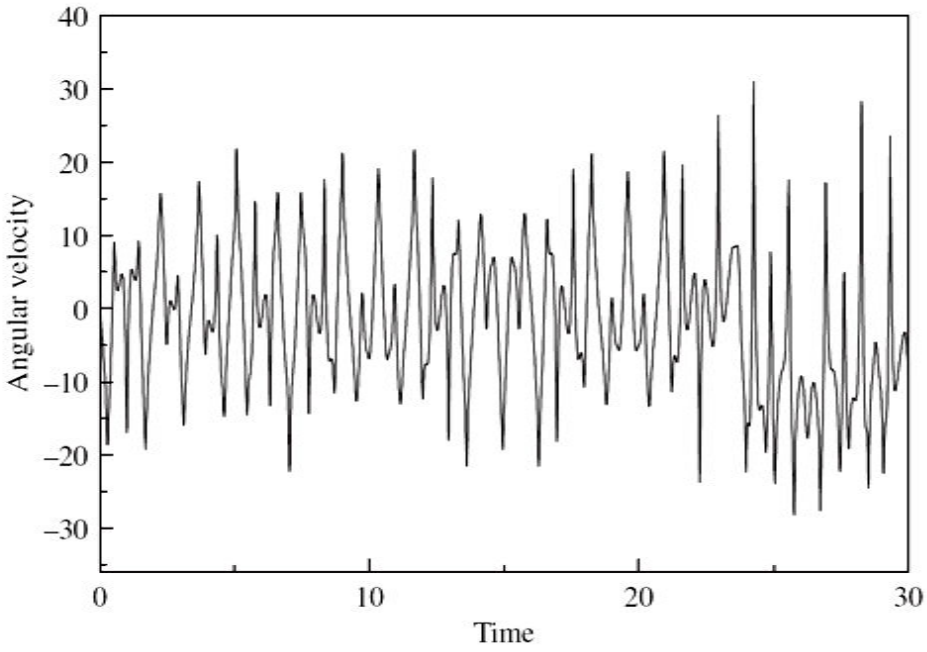

Fig. 5 Time series of the angular velocity of the lower mass of the double pendulum [1].

5. Introduction to dynamics

Phase space (definition 10, [2],[4])

Let us consider the following differential equations:

$$\frac{\mathrm{dx}}{\mathrm{dt}} = f(x), \qquad x(t_0) = x_0, \tag{5.1}$$

where $x \in D \subset \mathbb{R}^n, t \in \mathbb{R}^+$. D is open subset of $\mathbb{R}^n$. We call the system autonomus system of the n-th order, since time is not existent explicitely on right side of the given equation. For instance, free oscillations are considered as autonomous system, due to the fact that, energy is not delivered to the oscillated system. Analogously, the set of equations:

$$\frac{\mathrm{dx}}{\mathrm{dt}} = f(x,t), \qquad x(t_0) = x_0, \tag{5.2}$$

where $x \in D \subset \mathbb{R}^n, t \in \mathbb{R}^+$, in which time is given implicitly on the right side of the equation. Such a system is called nonautonomous system of the n-th order. The typical example of this system are oscillations with external excitation, wherein energy is delivered to the system. If there exists such $\mathrm{T} > 0$, that:

$$f(x,t) = f(x,t+T), \tag{5.3}$$

for every x and t, then the set of equations is called periodical, with period equal to T.

Nonautonomous, periodical set of equations of n-th order and period T can always be replaced with autonomous system of (n+1)-th order, under the condition that, additional variable $\theta = \frac{2\pi t}{T}$ is introduced. Then, the corresponding autonomous system has the following form:

$$\frac{\mathrm{dx}}{\mathrm{dt}} = f\left(x, \theta\left(\frac{t}{2\pi}\right)\right), \qquad x(t_0) = x_0\,; \tag{5.4}$$

$$\frac{\mathrm{d}\theta}{\mathrm{dt}} = \frac{2\pi}{\mathrm{T}}, \qquad \theta(t_0) = \frac{2\pi t_0}{T}. \tag{5.5}$$

The set D is called phase space of the system. In most of the considered systems, the phase space is n-th dimensional real space or its subspace, in the theory of oscillations.

The dynamic system defined by the equation (5.1) is such a mapping:

$$\Phi: \ \mathbb{R}^+ \times D \ \rightarrow \ \mathbb{R}^n, \tag{5.6}$$

defined by the solution $x(t)$ of the mentioned set of equations. The right side of this equation is a function f, defining vector field in $\mathbb{R}^n$:

$$f: \ \mathbb{R}^n \rightarrow \ \mathbb{R}^n. \tag{5.7}$$

In order to show the dependency of the autonomous system equation on the initial conditions in the explicit form, the solution is written in the form $\phi_t(x_0)$ frequently. The phase flux is represented by the mapping:

$$\Phi_\mathrm{t}: \ \mathbb{R}^n \rightarrow \ \mathbb{R}^n. \tag{5.8}$$

According to [2], the phase space of the dynamic system is an abstract space with orthogonal coordinates. Each coordinate represents parameter necessary to define the state of the system, for example, in order to define state of a particle moving rectilinearly we need to variables – x for the position and $\dot{x}$ for the velocity. Hence, phase space is 2 dimensional. However, if the particle is in uniform rectilinear motion, then to define its state, only 1 variable is sufficient – x, and as the consequence the phase space is 1 dimensional. Generally, the phase space of the dynamic system is $n-$ dimensional, depending on the dimension of the system.

Let us consider harmonic oscillator, characterised by the following equation:

$$\ddot{x} + x = 0, \tag{5.9}$$

with initial conditions $x(0) = x_0$ and $\dot{x}(0) = \dot{x}_0$. In order to receive set of equation, given by (5.1), we introduce new variables $x = x_1$ and $\dot{x} = x_2$, obtaining:

$$\dot{x}_1 = x_2, \tag{5.10}$$

$$\dot{x}_2 = -x_1. \tag{5.11}$$

Then, the solution of the equation (5.9) has the following form:

$$x_1 = x_0\, cos(t) + \dot{x}_0\, sin(t), \tag{5.12}$$

$$x_2 = -x_0\, sin(t) + \dot{x}_0\, cos(t). \tag{5.13}$$

Hence, the dynamic system defined by the equation (5.9) is given by the following mapping:

$$\Phi\left(t, x_{0,}\, \dot{x}_0\right) = \left(\, t, x_0\, cos(t) + \dot{x}_0\, sin(t)\,, -x_0\, sin(t) + \dot{x}_0\, cos(t)\,\right), \tag{5.14}$$

where:

$$\Phi : \ \mathbb{R}^+ \times \mathbb{R}^2 \to \mathbb{R}^2. \tag{5.15}$$

The solution of the equation (5.9) might be represented in 3 dimensional space $\mathbb{R}^+ \times \mathbb{R}^2$, as depicted in figure 6.

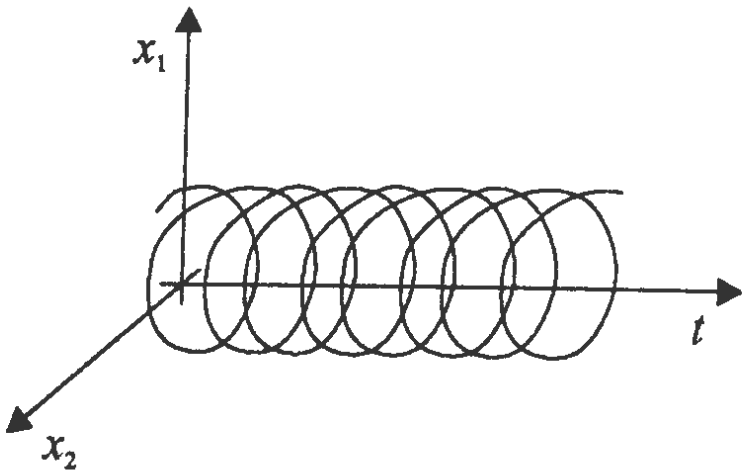

Fig. 6 Graphical representation of solution of the harmonic oscillator equation.

Dividing the equation (5.11) by (5.10), we receive:

$$\frac{dx_2}{dx_1} = -\frac{x_1}{x_2}, \tag{5.16}$$

and after integrating (5.16), we receive equations forming set of circles in phase space $\mathbb{R}^2$:

$$x_1^2 + x_2^2 = c, \tag{5.17}$$

$$c = (x_1(0))^2 + (x_2(0))^2. \tag{5.18}$$

And its graphical representation in figure 7:

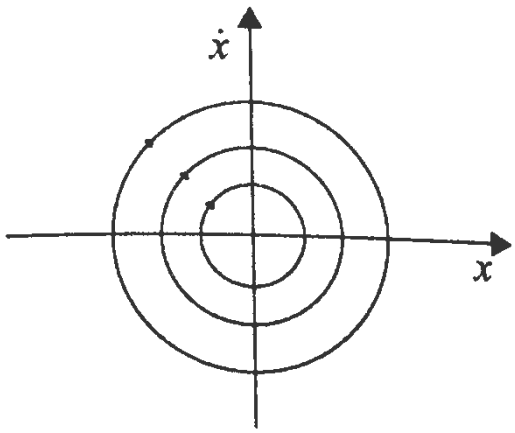

Fig. 7 Set of circles in phase space R^2.

Trajectory (definition 11, [4])

The equation analogical to the (5.16) can be written for general case, defined by the set of equations (5.1). One can present mentioned set in the following form:

$$\frac{dx_i}{dt} = f_i(x), \qquad i = 1, 2, \dots, n. \tag{5.19}$$

If $f_1(x) \neq 0$, then it is possible to replace componential part x_1 of the vector x with a new independent variable. In such a case we obtain:

$$\frac{dx_2}{dt} = -\frac{f_2(x)}{f_1(x)},$$

...

$$\frac{dx_n}{dt} = \frac{f_n(x)}{f_1(x)}.$$

(5.20)

The solution of the equations (5.20) in phase space is called trajectory (orbit) of the system. According to the theorem of existence and explicity of the solution of the differential equation, phase trajectories cannot intersect.

Critical point (definition 12, [4])

In order to receive equations (5.21) it is considered that $f_1(x) \neq 0$. However, if $f_1(x) = 0$ and $f_2(x) \neq 0$, then as the independent variable x_2 should be chosen. if $f_2(x) = 0$ and $f_3(x) \neq 0$, then variable x_3 should be chosen, etc. As shown, this construction is impossible in points $a = (a_1, \dots, a_n) \in \mathbb{R}^n$, such that:

$$f_1(a) = f_2(a) = \dots = f_n(a) = 0,$$

(5.21)

The point such that $a \in \mathbb{R}^n$ and $f(a) = 0$ is called the critical point of the set of equations (5.1). The critical point corresponds to the equilibrium position of the dynamic system, while it can be verified, that $x(t) = a$ fulfills equations of motion for every value of t [4].

Attractor (definition 13, [4],[9])

An attractor of a dynamical system is a subset of the state space to which orbits originating from typical initial conditions tend as time increases. For dynamical systems it is very frequent to have more than one attractor. For each such attractor, its basin of attraction is the set of initial conditions leading to long-time behaviour that approaches that attractor. Thus the qualitative behaviour of the long-time motion of a given system can be fundamentally different depending on which basin of attraction the initial condition lies in (e.g., attractors can correspond to periodic, quasiperiodic or chaotic behaviours of different types). Regarding a basin of attraction as a region in the state space, it has been found that

the basic topological structure of such regions can vary greatly from system to system.

Let us consider the following equation:

$$\frac{\mathrm{dx}}{\mathrm{dt}} = -x^2, \qquad x(0) = x_0. \tag{5.22}$$

It can be proved, that $x = 0$ is the critical point and $x(t) = 0$ is the equilibrium position. For $x_0 \neq 0$ the equation (5.22) has the solution in form:

$$x(t) = \left(\frac{1}{x_0} + t\right)^{-1}, \tag{5.23}$$

which is different for $x_0 > 0$ and $x_0 < 0$. For the case $x_0 > 0$, we have :

$$\lim_{t\to\infty} x(t) = 0. \tag{5.24}$$

Whereas for $x_0 < 0$ the solution is unbounded (fig. 8).

The above example has proved that, for $x_0 > 0$ the solution is tending to the critical point, when time is going to infinity. Such a phenomena is called attraction and the subset of the phase space, towards which solution of system is heading for, is called attractor.

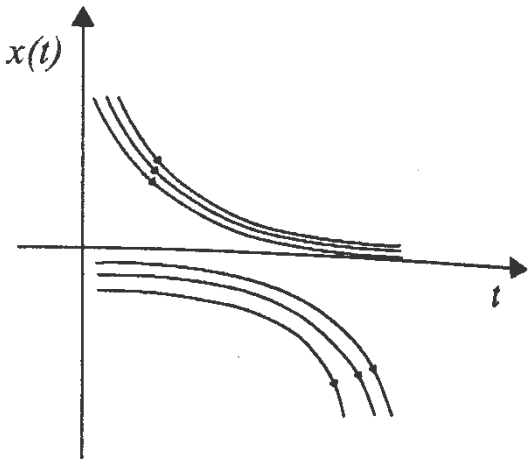

Fig. 8 Unbounded solution.

Limit cycle (definition 14, [4])

Let us consider the general case, when $x = \Phi(t)$ is the solution of the set of equations given by (5.1) and let us introduce the constant T, such that:

$$\Phi(t) = \Phi(t+T), \tag{5.25}$$

for every t, then $\Phi(t)$ is called periodic solution of period T. A closed curve in the phase space corresponds to the periodic solution.

The periodic solutions of the autonomous system are also called limit cycles (see fig. 12, chapter 6.1). If the limit cycle is attainable by the solution, when $t \to \infty$, then it is stable and it is the attractor. Whereas, when the limit cycle has this feature for $t \to -\infty$, then it is unstable and is unstable attractor [4].

Periodic function (definition 15, [10])

A function $f(x)$ is said to be periodic, with period p, if:

$$f(x) = f(x+np), \tag{5.26}$$

for $n = 1, 2, \ldots, n$.

Quasiperiodic function (definition 16, [6])

The quasiperiodic function is called such a function:

$$u(t) = F(\omega_1 t, \ldots, \omega_n t), \tag{5.27}$$

where: $F : \mathbb{R}^n \to \mathbb{R}$, is 2π-periodic function considering every variable, and frequencies $\omega_j, j = 1, \ldots, n$ are independent, i.e satisfying the relation:

$$\sum_{j=1}^{n} a_j \omega_j = 0, \qquad a_j \in \mathbb{Q}, \ j = 1, \ldots, n \quad \Rightarrow \quad a_j = 0, \qquad j = 1, \ldots, n \ . \tag{5.28}$$

Chaotic function (definition 17, [11])

Let us consider the following representations:

(X, d) - metric space

$S : X \longrightarrow X$ - continuous function

(X, S) – dynamic system with discrete time

X - phase space

S - dynamic of system (X, S)

$\{S_n(x)\}_{n \in N} = \{x, S(x), S^2(x), \dots\}$ - trajectory of points $x \in X$

Point $x \in X$ is called periodic, of period $n \in N$, $n \geq 2$, if $S^n(x) = x$ and $S^k(x) \neq x$ for $k = 1,2, \dots, n-1$.

The dynamic system (X, S) is called chaotic and dynamic S is called chaotic function, if the following assumptions are fulfilled:

- transitivity (T)
- sensitivity (W)
- density of periodic points (O)

- <u>Transitivity (T)</u>

The dynamic system (X, S) has the transitivity feature (T), if for an arbitrary pair of nonempty and open sets A, B in X, there exists number $n \in N$, such that: $S^n(A) \cap B \neq 0$.

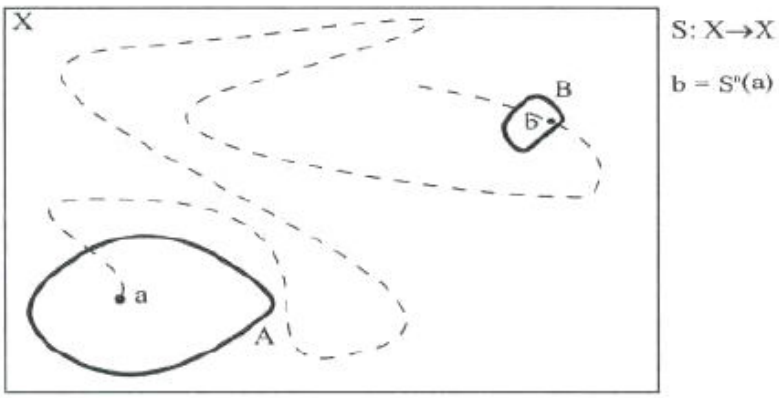

Fig. 9 Transitivity.

- Density of periodic points (O)

The dynamic system (X, S) has the feature of density of periodic points, if periodic points of dynamic S create dense subset of X.

Fig. 10 Density of periodic points.

- Sensitivity (W)

The dynamic system (X, S) is said to be sensitive, if there exists such a number $\delta > 0$, that for every $x \in X$ and its neighbourhood O_x, there is $y \in O_x$ and $n \geq 0$, such that:
$d(S^n(x), S^n(y)) > \delta$.

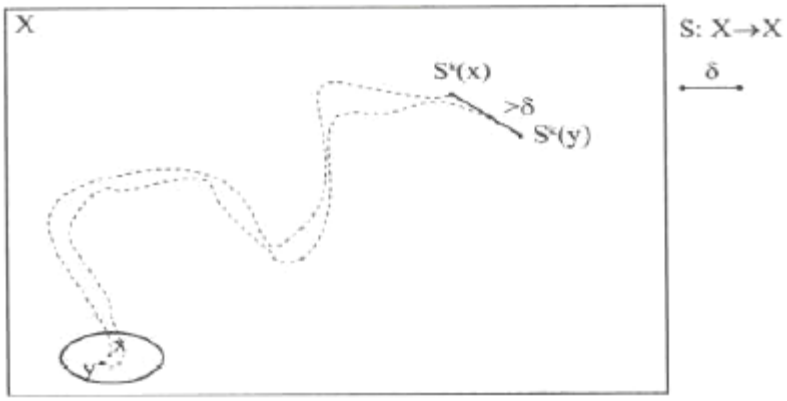

Fig. 11 Sensitivity.

6. Investigation tools of nonlinear dynamics

As the tools for chaos detection Poincaré maps and bifurcation diagrams are used. Both described below according to [2],[3],[4].

6.1 Poincaré maps

The theoretical base for Poincaré maps was introduced by Jules Henri Poincaré [3]. The widespread use of computer graphics facilities to examine chaotic behaviour in dynamical systems has led to the method of Poincaré maps becoming one of the most popular and the most illustrative method of describing 'strange attractors'.

During investigations of the dynamical system we are particularly interested in the asymptotic behaviour of the phase trajectories. This allows us to investigate the behaviour of the phase trajectories points of the specially selected time periods. The Poincaré maps consists of these points.

The definition of Poincaré map is different for autonomous and nonautonomous systems. At first, let us assume, that considered dynamical system is defined by the equation:

$$\frac{dx}{dt} = f(x), \qquad x \in \mathbb{R}^n, \tag{6.1}$$

and has limit cycle, as depicted in figure 12. Let x^* be the point placed at the limit cycle and $\sum$ is the (n-1)-dimensional area, throughout which limit cycle is cut in point x^*. Phase trajectory beginning at point x cuts again the area $\sum$ after time interval equal to period of limit cycle T. Phase trajectories starting in the vicinity of point $x^* - U$, placed on the area $\sum$, after period T cut the area in vicinity of $x^* - V$. Hence, equation of motion (6.1) and the area $\sum$ define mapping P, characterising vicinity $U \subset \sum$ of point x^* onto vicinity V of point x^*. Such a mapping is denoted as Poincaré map for autonomous system.

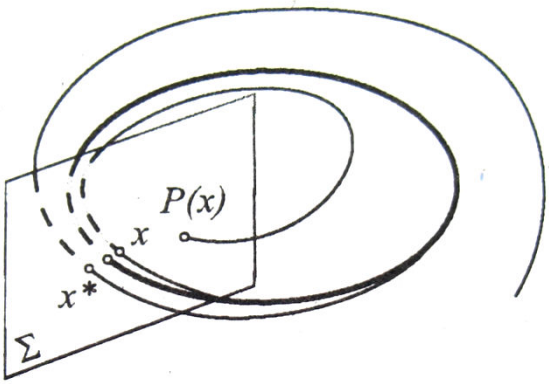

Fig. 12 Limit cycle.

Let us consider dynamic system, defined by the following equation:

$$\frac{dx}{dt} = f(x), \qquad x \in \mathbb{R}^3. \tag{6.2}$$

The Poincaré map may be defined as the set:

$$\left\{ \left(x_1(t),\, x_2(t)\right)\big|_{\,t=t_k} \right\}, x_3(t_k) = const. \tag{6.3}$$

Having defined the Poincaré map in such a manner we cannot assume it is done properly, since the phase trajectory can never transect area $\sum$ (for instance $\sum_3$ in figure 13). In actual euclidean phase space for dynamic system, having the attractor different than critical point, there is a possibility to specify $\sum$ in such a manner, that Poincaré map is defined properly [4].

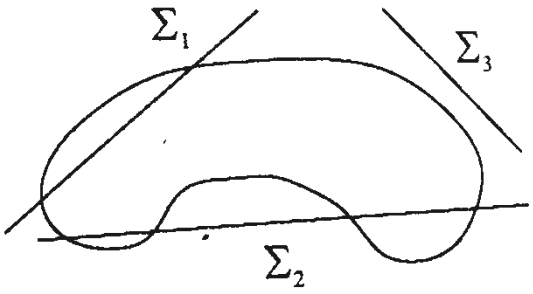

Fig. 13 Phase trajectory transecting areas $\sum_1$ and $\sum_2$.

It should be taken into consideration, that Poincaré map obtained according to the above rules is not interchangeable construction. It may happen that, trajectory

never transects specified area $\sum$, since for the dynamic system given, there are many possible choices for $\sum$, as shown in figure 13.

Let us define the Poincaré map for nonautonomous systems, given by:

$$\frac{dx}{dt} = f(x,t)\,, \qquad x \in \mathbb{R}\,, \tag{6.4}$$

where $f(x,t)$ is periodic function characterised by period T. The system specified by equation (6.4) might be denoted as $(n+1)$-dimensional autonomous system of cylindrical phase space $\mathbb{R}^n \times S^1$.

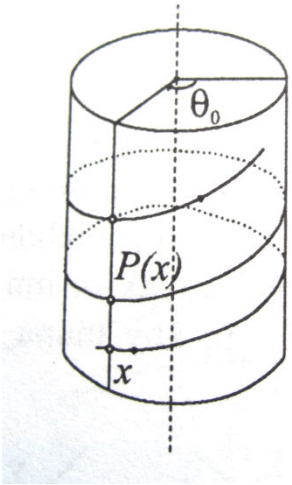

Fig. 14 Cylindrical phase space.

Considering n-dimensional area $\sum \in \mathbb{R}^n \times S^1$:

$$\sum = \{\,(x\,,\theta) \in \mathbb{R}^n \times S^1, \qquad \Theta = \Theta_0\,\}. \tag{6.5}$$

After time equal to the period T, phase trajectory $x(t)$ transects area $\sum$ (fig. 14). The mapping defined as:

$$P : \Sigma \to \Sigma \;(\,\mathbb{R}^n \to \mathbb{R}^n\,), \tag{6.6}$$

and mapping $x(t)$ in $x(t+T)$ is called Poincaré map.

6.2 Bifurcations

A concept of bifurcations was introduced into nonlinear dynamics by Poincaré. Bifurcation indicates a qualitative change of the features of a dynamical system, such as the solution of nonlinear differential equation that describes the system. Let us consider the following, nonlinear differential equation:

$$\frac{dx}{dt} = f(x, a), \tag{6.7}$$

where $x \in \mathbb{R}^n$, $a \in \mathbb{R}$. The bifurcation takes place, when the solution of the above equation qualitatively changes its character according to changes of the parameter a. The magnitude of $a = a_c$, for which this change occurs is called bifurcation point (locations at which bifurcations occur, that are in the state-control space, formed by state variables and control parameters). By definition local bifurcation is a qualitative change occurring in the neighbourhood of a fixed point or a periodic solution of the system. Any other qualitative change is known as global bifurcation. Generally, it is said, that the theory of bifurcation is the science investigating how the number or character of attractors of the equation (6.7) changes in relation to changes of parameter a [3].

Basically, bifurcations are divided into continuous and discontinuous (sometimes called catastrophic) bifurcations. The division depends on the continuous or discontinuous variation of the state of the system , when the control parameter is changed gradually, through its critical value. In continuous-time systems, such as defined by (6.7), when at least one of the control parameters corresponding to a stable fixed point is altered , the fixed point may lose its stability through one of the following bifurcations:

- pitchfork bifurcation
- transcritical bifurcation
- saddle-node bifurcation
- Hopf bifurcation.

The first three types of bifurcations are classified as the static ones, while at the bifurcation points related to them, only branches of fixed points or static solutions meet. Considering the Hopf bifurcation, branches of fixed points and branches of periodic solutions meet, and that is why these bifurcations are defined as dynamical.

Below, types of bifuractions are presented, basing on [2].

6.2.1 Pitchfork bifurcation

Let us investigate the bifurcation occurring in the dynamical system, described by the following equation:

$$\frac{dx}{dt} = ax - bx^3, \tag{6.8}$$

where a, b are real constants. It can be proved, that points:

$$x = 0 \qquad \text{for} \qquad a \in \mathbb{R},$$

as well as

$$x = \pm\sqrt{\frac{a}{b}},$$

for

$$a, b \in \mathbb{R}, \frac{a}{b} > 0,$$

are the critical points of the equation (6.8).

In order to investigate stability of the point $x = 0$, let us consider the linearised equation:

$$\frac{dx}{dt} = ax. \tag{6.9}$$

The solution of the above equation takes the following form:

$$x(t) = x_0 e^{a\,t},$$

where $x_0 = x(0)$ is the initial condition. Hence, one receives, that $x = 0$ is the stable critical point, under the condition that $a \leq 0$.

The nonlinear equation (6.9) can be solved substituting $1/x^2$ for x. Then, the linear equation, with respect to $1/x^2$ is obtained:

$$\frac{1}{x^3}\frac{dx}{dt} = \frac{a}{x^2} - b \tag{6.10}$$

or

$$\frac{dx^{-2}}{dt} + 2ax^{-2} = 2b, \tag{6.11}$$

with the solutions formulated as follows:

$$x^2(t) = \begin{cases} \dfrac{ax_0^2}{bx_0^2 + (a - bx_0^2)e^{-2at}} \\ \dfrac{x_0^2}{1 + 2bx_0^2 t} \end{cases},$$

for a,

or

$$x(t) = \sqrt{x^2(t)}\, sgn(x_0),$$

where $sgn\, x_0 = 1$, for $x_0 > 0$, $sgn\, x_0 = -1$ $x_0 < 0$, $sgn\, x_0 = 0$ $x_0 = 0$.

The bifurcation takes place at point $a = 0$. There exists one stable critical point (attractor) $x = 0$, for $a \leq 0$. Whereas, when $a > 0$, there exist 2 stable critical points (attractors) $x = \pm\sqrt{a/b}$ and nonstable critical point (negative attractor) $x = 0$. Such a bifurcation is called supercritical, since new qualitative solution occurs for $a > a_c$.

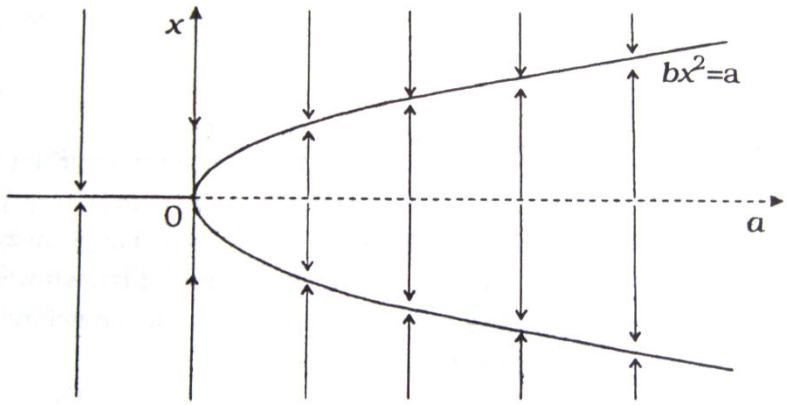

Fig. 15 Supercritical bifurcation.

For $a \geq 0$ there exists only 1 unstable critical point $x = 0$, whereas for $a \leq 0$, there are 3 stable points $x = 0$ and unstable $x = \pm\sqrt{a/b}$. Such a bifurcation is called subcritical.

Bifurcations presented in figures 15 and 16, are called pitch-fork bifurcations.

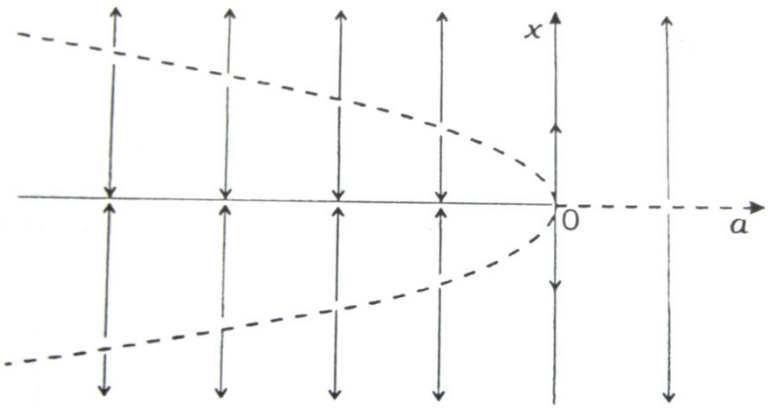

Fig. 16 Subcritical bifurcation.

6.2.2 Saddle-node bifurcation

The another type of bifurcation is described by means of the following equation:

$$\frac{dx}{dt} = a - x^2. \tag{6.16}$$

The critical point of above equation are

$$x_1 = \sqrt{a}, \qquad x_2 = -\sqrt{a}.$$

While we are interested in real solutions only, we see, that for a > 0 we have 2 critical points, for a $= 0$, and there are none for a < 0. Equation (6.16) can be integrated using variable division.

$$x(t) = \begin{cases} \sqrt{a}\,\dfrac{x_0 + \sqrt{a}\tanh(\sqrt{a}t)}{\sqrt{a} + x_0\tanh(\sqrt{a}t)} & for\ a > 0 \\ \dfrac{x_0}{1 + x_0 t} & for\ a = 0 \\ \sqrt{-a}\,\dfrac{x_0 - \sqrt{-a}\tanh(\sqrt{-a}t)}{\sqrt{-a} + x_0\tanh(\sqrt{-a}t)} & for\ a < 0 \end{cases}. \tag{4.17}$$

In the above equation, as the initial condition $x_0 = x(0)$ is taken. Analysing the course of the function of the solution of $x(t)$ we see, that:

$$\lim_{t \to \infty} x(t) = \sqrt{a} \qquad for\ a > 0 \quad and \quad x_0 > -\sqrt{a},$$

$$\lim_{t \to \infty} x(t) = -\sqrt{a} \qquad for\ a > 0 \quad and \quad x_0 > -\sqrt{a},$$

$$\lim_{t \to \infty} x(t) = 0 \qquad for \quad a = 0 \quad and \quad x_0 \geq 0,$$

Moreover,

$$\lim_{t \to \frac{1}{x_0}} x(t) = -\infty \quad for\ a = 0\ and\ x_0 < 0,$$

$$\lim_{t \to \sqrt{a}\tanh(\frac{-\sqrt{a}}{x_0})} x(t) = -\infty \quad for\ a > 0\ and\ x_0 < -\sqrt{a},$$

$$\lim_{t \to \sqrt{-a}\tanh(\frac{-\sqrt{-a}}{x_0})} x(t) = +\infty \quad for\ a < 0.$$

The properties of the solution (6.16) are presented in figure below.

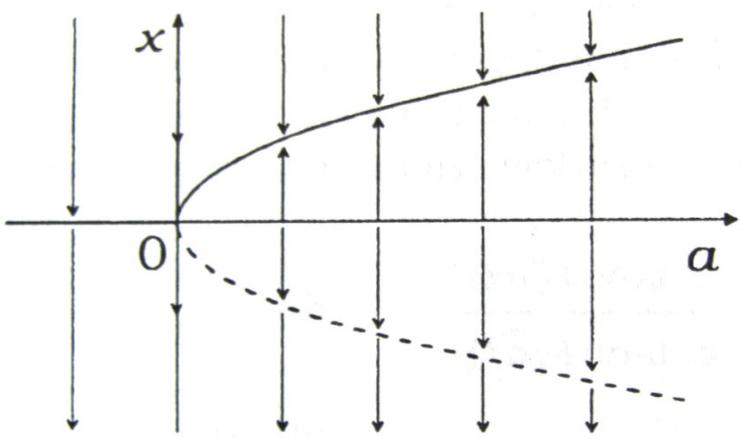

Fig. 17 Illustration of the properties of the equation (6.16).

This elaboration implies, that number of critical points is changing, when the value of parameter a passes zero. Moreover, stability of critical points is also changing, when $x = \pm\sqrt{a}$ passes zero. This kind of bifurcation is called saddle-node bifurcation.

6.2.3 Hopf bifurcation

The Hopf bifurcation lies in loss of the stability of the critical point, what implies appearance of periodic solution (limit cycle). The bifurcation can be discussed using the following set of differential equations:

$$\frac{dx}{dt} = -y + (a - x^2 - y^2)x,$$

$$\frac{dy}{dt} = x + (a - x^2 - y^2)y,$$

(6.18)

where $a \in \mathbb{R}$. Assuimng $dx/dt = dy/dt = 0$, it can be seen, that $x = 0$ and $y = 0$ are the critical points. Linearising (6.18) in the neighbourhood of the critical point, one obtains:

$$\frac{dx}{dt} = -y + ax,$$

$$\frac{dy}{dt} = x + ay.$$

(6.19)

The solution of the above set of equation is combination of the linear functions:

$$x(t) = e^{\lambda t}u,$$

$$y(t) = e^{\lambda t}v,$$

satisfying the equation:

$$A\,u = s\,u,$$

where s is proper value, $u = [u, v]^T$, are the proper vectors, and A is 2×2 matrix:

$$A = \begin{bmatrix} a & -1 \\ 1 & a \end{bmatrix}.$$

Hence,

$$0 = \det(A - s) = \begin{vmatrix} a - s & -1 \\ 1 & a - s \end{vmatrix} = (a - s)^2 + 1,$$

yielding

$$s = a \pm i. \tag{6.20}$$

The solution $y = x = 0$ of the linearised system is stable, if $Re(s_{1,2}) < 0$, i. e. when $a < 0$ and unstable for $a > 0$.

The form of the set of equations (6.18) was chosen in such a manner, that they are able to be solved analytically. Introducing polar coordinates $x = r\,cos\theta, y = r\,sin\theta$ for $r \geq 0$ it can be easily shown, that $x + iy = r\,exp(\mathrm{i}\theta)$. Multiplying the second equation from the set (6.18) by i and then adding to the first one, one receives:

$$\frac{d(r\,e^{i\theta})}{dt} = \frac{dx}{dt} + i\frac{dy}{dt} = -y + ix + (a - x^2 - y^2),$$

or

$$\left(\frac{dr}{dt} + ir\frac{d\theta}{dt}\right)e^{i\theta} = ire^{i\theta} + (a - r^2)re^{i\theta}. \tag{6.21}$$

Dividing both sides of the above equation by $exp(i\theta)$ and comparing real and imaginary parts on the both sides of the equation, we obtain:

$$\frac{dr}{dt} = r(a - r^2),$$

$$\frac{d\theta}{dt} = 1. \tag{4.22}$$

Hence,

$$r^2(t) = \begin{cases} \dfrac{ar_0^2}{r_0^2 + (a - r_0^2)e^{-2at}} & for\ a \neq 0 \\ \dfrac{r_0^2}{1 + 2r_0^2 t} & for\ a = 0 \end{cases}, \tag{6.23}$$

and

$$\theta = t + \theta,\ \ r_0 = r(0),\ \ \theta_0 = \theta(0).$$

The solution (6.23) can be presented as the phase trajectory $x = (x(t), y(t))$ on the plane, introducing Cartesian coordinate system $x - y$. For $a \leq 0$, all phase trajectories $x(t) \to 0$ for $t \to \infty$ and point x (0,0) is the attractor. The behaviour of phase trajectories in that case are presented below.

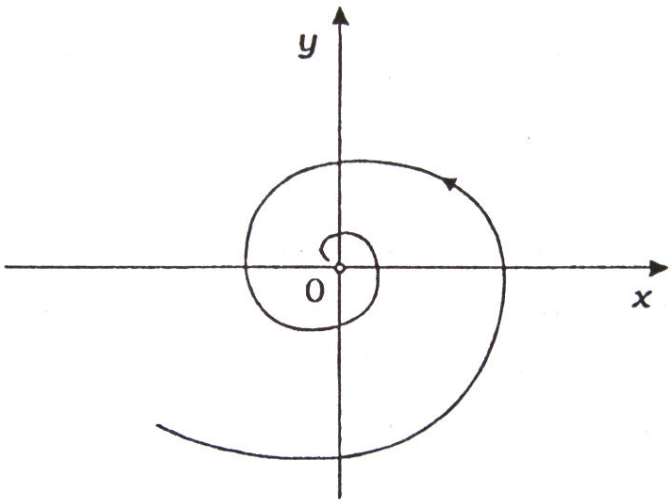

Fig. 18 Phase trajectories of the solution (6.23).

For $a > 0$ point x (0,0) becomes the negative attractor and as the consequence new stable solution appears:

$$x = \sqrt{a}\cos(t + \theta_0),$$

$$y = \sqrt{a}\sin(t + \theta_0),$$

which is limit cycle. Such a solution is shown in figure 19.

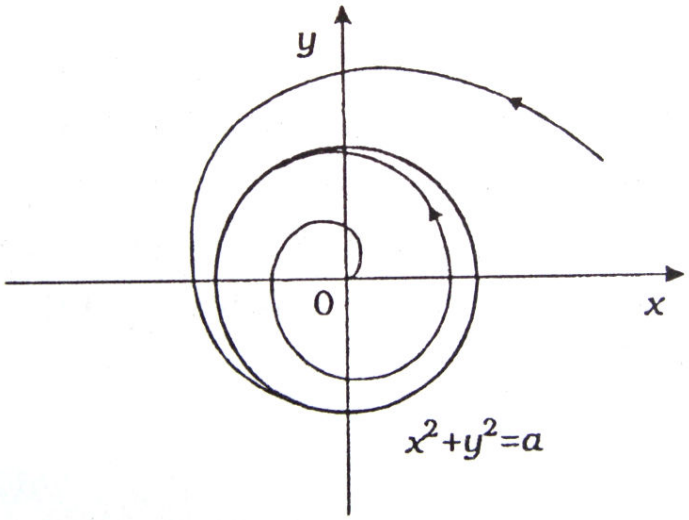

Fig. 19 Limit cycle for negative attractor.

All phase trajectories beginning at the arbitrary point of the phase space, other than x (0,0) tend to periodic trajectory, in our case described by the equation:

$$x^2 + y^2 = a.$$

The presented Hopf bifurcation is the supercritical bifurcation, i.e the stable limit cycle replaces stable critical point, when a changes sign.

As shown, in case of transcritical bifurcation or pitch-fork bifurcation, the real proper value passes zero as parameter a passes critical value (for instance a_0), either increasing or decreasing. See figure below.

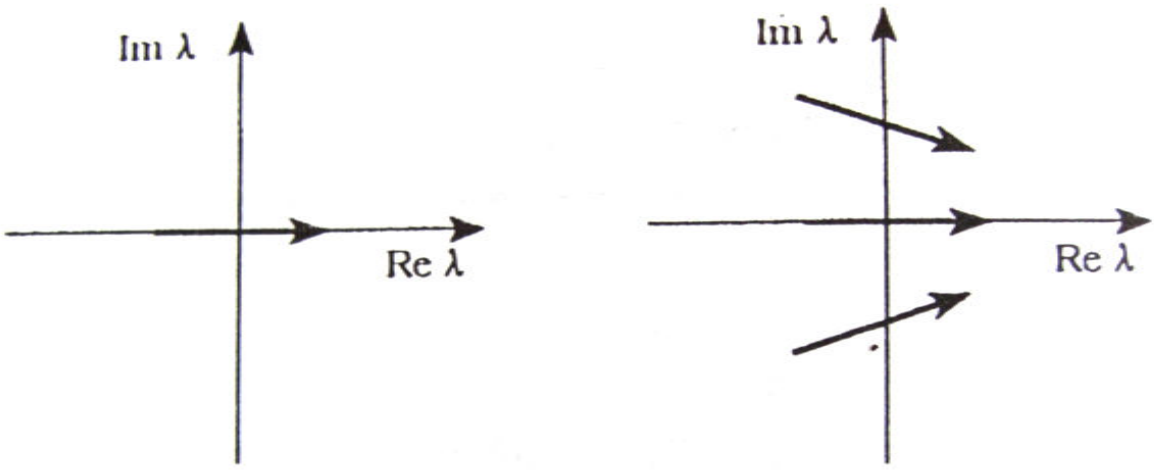

Fig. 20 Left: Saddle-node bifurcation; Right: Hopf bifurcation.

As the consequence of this transition, one or two stable critical points emerge. On the contrary to these bifurcations, in case of Hopf bifurcations, the real part of the conjugated proper values $\lambda_{1,2}$ changes sign from negative to positive and when passes critical value a_0 the stable critical point is replaced with the limit cycle.

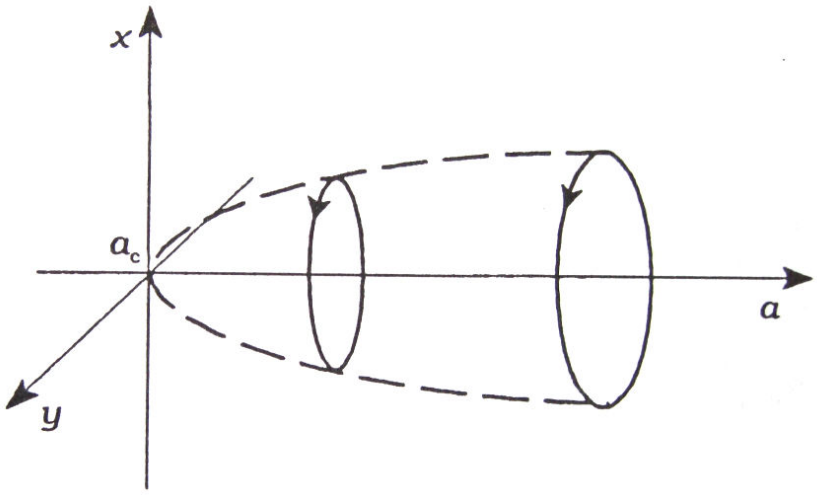

Fig. 21 Replacement of stable critical point with the limit cycle.

Hopf bifurcations are characteristic for number of nonlinear differential equations.

7. Model of the double pendulum

While the topic of this thesis concerns the investigation and analysis of the motion of the double pendulum system using numerical methods only, all relevant physical phenomena have to be presented using language of mathematics. At first, the general case will be introduced, basing on which, the special case of the double pendulum system will be derived. The latter case is related to the model of investigation of this paper, including all necessary specification and requirements.

At the very beginning, there will be thorough study of the possible positions occupied by the system, followed by projecting those positions on coordinate system. Knowing that, velocities will be found. The next step is to define potential and kinetic energy of the system, as well as finding their proper derivatives, which will make it possible to formulate equations of motion, on the basis of Lagrangian mechanics.

7.1 The general case

Let us consider a model of plane (2 dimensional), double pendulum, attached to the tie, as depicted in figure 22. The system consists of 2 elastic and weightless joints – 2 springs of characteristics k_1 and k_2.

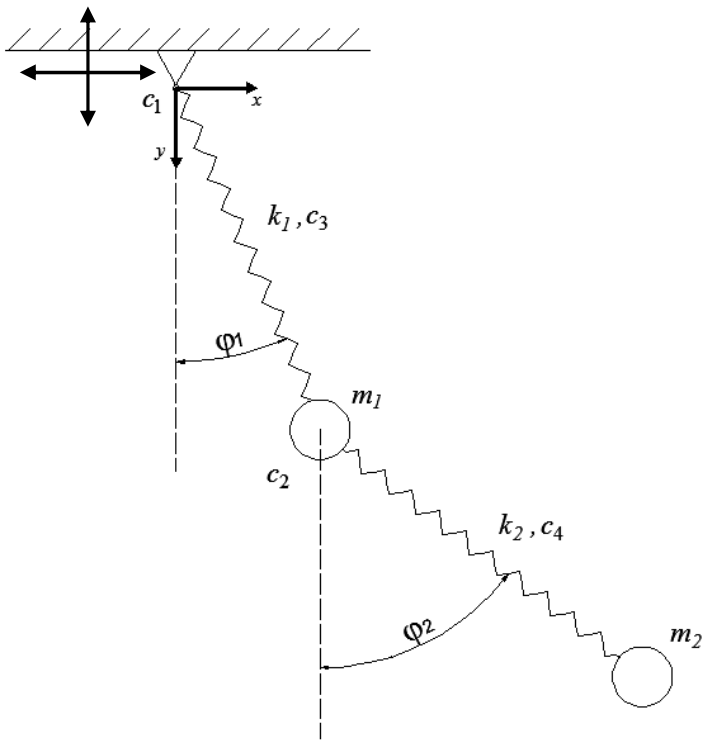

Fig. 22 General case of double pendulum.

There are point masses m_1 and m_2 fastened to the ends of particular joints of initial length l_{01} and l_{02}, respectively. Since both springs are stretched by the point masses, considering l_{01}, l_{02} as the initial lengths, their total lengths at rest can be formulated as follows:

$$l_I = l_{01} + \frac{(m_1 + m_2)g}{k_1}, \tag{7.1}$$

$$l_{II} = l_{02} + \frac{m_2 g}{k_1}. \tag{7.2}$$

While swinging, since dynamic forces are applied, springs elongate further and their total lengths are l_1 and l_2, respectively. Due to the viscous damping at the fastenings and in springs occur, viscous damping coefficients c_1 and c_2 for the fastenings and c_3 and c_4 for the springs need to be introduced.

The whole system is subjected to the circular excitation E, which can be decomposed to the horizontal and vertical components:

$$E_x = A\ sin\ \omega t, \tag{7.3}$$

$$E_y = A\ cos\ \omega t, \tag{7.4}$$

and its derivatives are as follows:

$$\dot{E}_x = A\omega\ cos\ \omega t, \tag{7.5}$$

$$\dot{E}_y = -A\omega\ sin\ \omega t, \tag{7.6}$$

$$\ddot{E}_x = -A\omega^2\ sin\ \omega t, \tag{7.7}$$

$$\ddot{E}_y = -A\omega^2\ cos\ \omega t. \tag{7.8}$$

Using the Lagrangian mechanics, the equations of motion will be derived. The generalised coordinates are φ_1 , φ_2 and l_1 , l_2. Projecting the positions of the pendulum`s masses on the Cartesian coordinate system, shown in figure 22, we obtain:

$$r_{x1} = l_1 \sin\varphi_1 - E_x, \tag{7.9}$$

$$r_{x2} = l_1 sin\varphi_1 - E_x + l_2 sin\varphi_2, \tag{7.10}$$

$$r_{y1} = l_1 \cos\varphi_1 - E_y, \tag{7.11}$$

$$r_{y2} = l_1 cos\varphi_1 - E_y + l_2 cos\varphi_2.$$

(7.12)

By integrating and summing (7.9) and (7.11), as well as (7.10) and (7.12), we obtain equations of velocities:

$$v_1 = (\dot{l_1}^2 - 2\dot{l_1} sin\varphi_1 \dot{E_x} - 2l_1 cos\varphi_1 \dot{\varphi_1} \dot{E_x} + \dot{E_x}^2 - 2\dot{l_1} cos\varphi_1 \dot{E_y} + {l_1}^2 \dot{\varphi_1}^2 + 2l_1 sin\varphi_1 \dot{\varphi_1} \dot{E_y} + \dot{E_y}^2)^{\frac{1}{2}},$$

(7.13)

$$\begin{aligned} v_2 = (&-2l_1 cos\varphi_1 \dot{\varphi_1} \dot{E_x} + 2l_1 sin\varphi_1 \dot{\varphi_1} \dot{E_y} + 2l_1 \dot{\varphi_1} l_2 \dot{\varphi_2} \cos(\varphi_1 - \varphi_2) + \dot{l_2}^2 \\ &+ 2\dot{l_1} \dot{l_2} \cos(\varphi_1 - \varphi_2) + 2\dot{l_1} l_2 \dot{\varphi_2} \sin(\varphi_1 - \varphi_2) - 2\dot{\varphi_1} \dot{l_2} \sin(\varphi_1 - \varphi_2) \\ &+ {\dot{\varphi_2}}^2 {l_2}^2 - 2\dot{l_1} sin\varphi_1 \dot{E_x} - 2\dot{l_1} cos\varphi_1 \dot{E_y} + \dot{E_x}^2 + \dot{E_y}^2 + \dot{l_1}^2 + {l_1}^2 \dot{\varphi_1}^2 \\ &- 2\dot{E_x} l_2 cos\varphi_2 \dot{\varphi_2} + 2\dot{E_y} l_2 sin\varphi_2 \dot{\varphi_2} - 2\dot{E_x} \dot{l_2} sin\varphi_2 - 2\dot{E_y} l_2 cos\varphi_2)^{\frac{1}{2}}, \end{aligned}$$

(7.14)

According to definition 5, the total kinetic energy of the system is given by :

$$T = \sum_{i=1}^{n} \frac{m_i \vec{v}_i^2}{2}.$$

Substituting squares of (7.13) and (7.14) into (2.5), the total kinetic energy of the system is:

$$\begin{aligned} T = \frac{1}{2} m_1 \Big(&\dot{l_1}^2 - 2\dot{l_1} sin\varphi_1 \dot{E_x} - 2l_1 cos\varphi_1 \dot{\varphi_1} \dot{E_x} + \dot{E_x}^2 - 2\dot{l_1} cos\varphi_1 \dot{E_y} - {l_1}^2 \dot{\varphi_1}^2 \\ &+ 2l_1 sin\varphi_1 \dot{\varphi_1} \dot{E_y} + \dot{E_y}^2 \Big) \\ &+ \frac{1}{2} m_2 \Big(-2l_1 cos\varphi_1 \dot{\varphi_1} \dot{E_x} + 2l_1 sin\varphi_1 \dot{\varphi_1} \dot{E_y} + 2l_1 \dot{\varphi_1} l_2 \dot{\varphi_2} \cos(\varphi_1 - \varphi_2) \\ &+ \dot{l_2}^2 + 2\dot{l_1} \dot{l_2} \cos(\varphi_1 - \varphi_2) + 2\dot{l_1} l_2 \dot{\varphi_2} sin(\varphi_1 - \varphi_2) \\ &- 2l_1 \dot{\varphi_1} \dot{l_2} sin(\varphi_1 - \varphi_2) + {\dot{\varphi_2}}^2 {l_2}^2 - 2\dot{l_1} sin\varphi_1 \dot{E_x} - 2\dot{l_1} cos\varphi_1 \dot{E_y} + \dot{E_x}^2 \\ &+ \dot{E_y}^2 + \dot{l_1}^2 + {l_1}^2 \dot{\varphi_1}^2 - 2\dot{E_x} l_2 cos\varphi_2 \dot{\varphi_2} + 2\dot{E_y} l_2 sin\varphi_2 \dot{\varphi_2} - 2\dot{E_x} \dot{l_2} sin\varphi_2 \\ &- 2\dot{E_y} \dot{l_2} cos\varphi_2 \Big), \end{aligned}$$

(7.15)

whereas, potential energy (on the basis of definition 6), for the general case of double pendulum, takes the following form:

$$V = m_1 g l_1(1 - cos\varphi_1) + m_2 g\big(l_1(1 - cos\varphi_1) + l_2(1 - cos\varphi_2)\big) + \frac{1}{2}k_1(l_1 - l_I)^2 + \frac{1}{2}k_2(l_2 - l_{II})^2. \tag{7.16}$$

In order to calculate equations of motion, function of dissipation have to be also taken into consideration. For general case, it takes the following form:

$$D = \frac{1}{2}c_1\dot{\varphi_1}^2 + \frac{1}{2}c_2(\dot{\varphi_2} - \dot{\varphi_1})^2 + \frac{1}{2}c_3\dot{l_1}^2 + \frac{1}{2}c_4\dot{l_2}^2. \tag{7.17}$$

Having calculated (7.15), (7.16) and (7.17) and substituting their adequate derivatives to Lagrange`s equations of the 2nd kind (see chapter 2; 2.14), we receive 4 equations of motion for the system given in fig. 22; 1 equation for each degree of freedom. They are as follows:

$$\begin{aligned}\ddot{\varphi_1}(m_1 + m_2){l_1}^2 + \ddot{\varphi_2}m_2 l_1 l_2\, cos(\varphi_1 - \varphi_2) - \ddot{l_2}m_2 l_1 sin(\varphi_1 - \varphi_2) \\ + 2\dot{\varphi_1}\dot{l_1}l_1(m_1 + m_2) + 2\dot{\varphi_2}\dot{l_2}m_2 l_1\, cos(\varphi_1 - \varphi_2) \\ + \dot{\varphi_2}^2 m_2 l_1 l_2 \sin(\varphi_1 - \varphi_2) + (m_1 + m_2)g l_1 sin\varphi_1 \\ - \ddot{E_x}(m_1 + m_2)l_1 \cos\varphi_1 + \ddot{E_y}(m_1 + m_2)l_1 \cos\varphi_1 + c_1\dot{\varphi}_1 \\ + c_2(\dot{\varphi}_1 - \dot{\varphi}_2) = 0,\end{aligned} \tag{7.18}$$

$$\begin{aligned}\ddot{\varphi}_1 m_2 l_1 l_2 \cos(\varphi_1 - \varphi_2) + \ddot{\varphi}_2 m_2 {l_2}^2 + \ddot{l}_1\, m_2 l_2 \sin(\varphi_1 - \varphi_2) + \dot{\varphi}_1\dot{l}_1 m_2 l_2 \cos(\varphi_1 \\ - \varphi_2)\dot{\varphi}_1^{\,2} m_2 l_1 l_2 \sin(\varphi_1 - \varphi_2) + \dot{\varphi}_2\dot{l}_2 m_2 l_2 + m_2 g l_2 sin\varphi_2 \\ - \ddot{E_x}\, m_2 l_2 \cos\varphi_2 + \ddot{E_y} m_2 l_2 \sin\varphi_2 + c_2(\dot{\varphi}_2 - \dot{\varphi}_1) = 0,\end{aligned} \tag{7.19}$$

$$\begin{aligned}\ddot{\varphi}_2 m_2 l_2 \sin(\varphi_1 - \varphi_2) + \ddot{l}_1\,(m_1 + m_2) + \ddot{l}_2 m_2 \cos(\varphi_1 - \varphi_2) - \dot{\varphi}_1^{\,2} l_1(m_1 + m_2) \\ + 2\dot{\varphi}_2\dot{l}_2 m_2 \sin(\varphi_1 - \varphi_2) \; - \dot{\varphi}_2^{\,2} m_2 l_2 \cos(\varphi_1 - \varphi_2) + k_1(l_1 - l_I) + \; c_3\dot{l}_1 \\ + (m_1 + m_2)(1 - cos\varphi_1)g - \ddot{E_x}(m_1 + m_2)sin\,\varphi_1 \\ + \; \ddot{E_y}(m_1 + m_2)cos\,\varphi_1 = \; 0,\end{aligned} \tag{7.20}$$

$$\begin{aligned}-\ddot{\varphi}_1 m_2 l_1 \sin(\varphi_1 - \varphi_2) + \ddot{l}_1\, m_2 \cos(\varphi_1 - \varphi_2) + \ddot{l}_2 m_2 - 2\dot{\varphi}_1\dot{l}_1 m_2 sin(\varphi_1 \\ - \varphi_2) - \dot{\varphi}_1^{\,2} m_2 l_1 \cos(\varphi_1 - \varphi_2) - \dot{\varphi}_2^{\,2} m_2 l_2 \; + c_4\dot{l}_2 + k_2(l_2 - l_{II}) \\ + \; m_2 g(1 - cos\varphi_2) - \ddot{E_x} m_2 sin\,\varphi_2 - \ddot{E_y} m_2 cos\,\varphi_2 = 0.\end{aligned}$$

(7.21)

The general matrix representation of equations of motion can be presented in the following form:

$$M\ddot{q} + c\dot{q} + kq = f(t).$$

(7.22)

Rearranging equation (7.22), we obtain mass matrix M and rest matrix R in the following representation:

$$M\ddot{q} = R,$$

(7.23)

where:

$$\ddot{q} = M^{-1}R,$$

(7.24)

and

$$\ddot{q} = \begin{bmatrix} \ddot{\varphi}_1 \\ \ddot{\varphi}_2 \\ \ddot{l}_1 \\ \ddot{l}_2 \end{bmatrix}.$$

(7.25)

Putting equations (7.18), (7.19), (7.20) and (7.21) into (7.23), we obtain 4 dimensional system of equations of motion in matrix form, which is presented below:

$$\mathrm{M} = \begin{bmatrix} (m_1 + m_2){l_1}^2 & m_2 l_1 l_2 \cos(\varphi_1 - \varphi_2) & 0 & -m_2 l_1 \sin(\varphi_1 - \varphi_2) \\ m_2 l_1 l_2 \cos(\varphi_1 - \varphi_2) & \mathrm{m_2 l_2^2} & \mathrm{m_2 l_2 \sin(\varphi_1 - \varphi_2)} & 0 \\ 0 & \mathrm{m_2 l_2 \sin(\varphi_1 - \varphi_2)} & (\mathrm{m_1 + m_2}) & m_2 \cos(\varphi_1 - \varphi_2) \\ -m_2 l_1 \sin(\varphi_1 - \varphi_2) & 0 & m_2 \cos(\varphi_1 - \varphi_2) & m_2 \end{bmatrix}, \tag{7.26}$$

$$\ddot{q} = \begin{pmatrix} \ddot{\varphi}_1 \\ \ddot{\varphi}_2 \\ \ddot{l}_1 \\ \ddot{l}_2 \end{pmatrix}, \tag{7.27}$$

$$R = \begin{bmatrix} 2\dot{\varphi}_1 \dot{l}_1 l_1 (m_1 + m_2) + 2\dot{\varphi}_2 \dot{l}_2 m_2 l_1 \cos(\varphi_1 - \varphi_2) + \dot{\varphi}_2{}^2 m_2 l_1 l_2 \sin(\varphi_1 - \varphi_2) + (m_1 + m_2) g l_1 \sin\varphi_1 - \ddot{E}_x (m_1 + m_2) l_1 \cos\varphi_1 \\ + \ddot{E}_y (m_1 + m_2) l_1 \cos\varphi_1 + c_1 \dot{\varphi}_1 + c_2 (\dot{\varphi}_1 - \dot{\varphi}_2) \\ 2\dot{\varphi}_1 \dot{l}_1 m_2 l_2 \cos(\varphi_1 - \varphi_2) - \dot{\varphi}_1^2 m_2 l_1 l_2 \sin(\varphi_1 - \varphi_2) + 2\dot{\varphi}_2 \dot{l}_2 m_2 l_2 + m_2 g l_2 \sin\varphi_2 - \ddot{E}_x m_2 l_2 \cos\varphi_2 + \ddot{E}_y m_2 l_2 \sin\varphi_2 + c_2 (\dot{\varphi}_2 - \dot{\varphi}_1) \\ -\dot{\varphi}_1{}^2 l_1 (m_1 + m_2) + 2\dot{\varphi}_2 \dot{l}_2 m_2 \sin(\varphi_1 - \varphi_2) - \dot{\varphi}_2{}^2 m_2 l_2 \cos(\varphi_1 - \varphi_2) + k_1 (l_1 - l_I) + c_3 \dot{l}_1 + (m_1 + m_2)(1 - \cos\varphi_1) g \\ -\ddot{E}_x (m_1 + m_2) \sin\varphi_1 + \ddot{E}_y (m_1 + m_2) \cos\varphi_1 \\ -2\dot{\varphi}_1 \dot{l}_1 m_2 \sin(\varphi_1 - \varphi_2) - \dot{\varphi}_1{}^2 m_2 l_1 \cos(\varphi_1 - \varphi_2) - \dot{\varphi}_2{}^2 m_2 l_2 + c_4 \dot{l}_2 + k_2 (l_2 - l_{II}) + m_2 g (1 - \cos\varphi_2) - \ddot{E}_x m_2 \sin\varphi_2 - \ddot{E}_y m_2 \cos\varphi_2 \end{bmatrix}. \tag{7.28}$$

7.2 The examined system

In previous subchapter there was considered a generalised case of double pendulum. In this section, the special case will be analysed and all necessary derivations will be presented and then whole system will be verified in association with general case, performing all required modifications in general case model.

Let us have a look on a model of plane (2 dimensional), double pendulum, attached to a tie, as depicted in figure 23. The system consists of 2 weightless joints – the first on is elastic – spring with characteristic k_1, the second one is inelastic of fixed length.

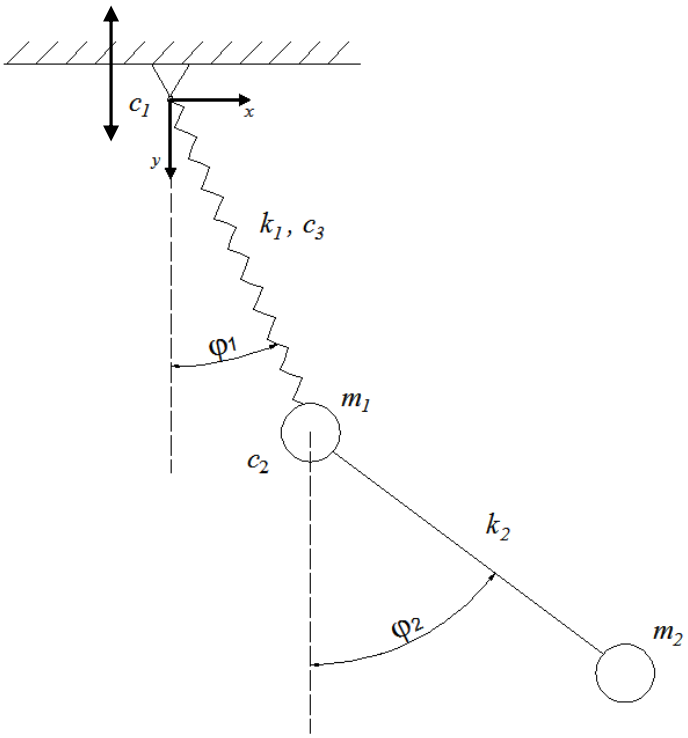

Fig. 23 Special case of double pendulum.

There are point masses m_1 and m_2 fastened to the ends of particular joints of initial length l_{01} and l_{02}, respectively. Since spring of the first joint is stretched by the point masses, the length at rest, taking l_{01} as the initial length, can be formulated as follows:

$$l_I = l_{01} + \frac{(m_1 + m_2)g}{k_1}. \tag{7.29}$$

While swinging, the length of the spring is increased, since dynamic forces are applied, and its total length is l_1. For convenience, let us denote length of the second joint as l_2 :

$$l_{02} = l_2. \tag{7.30}$$

Due to the viscous damping at the fastenings and in spring occur, viscous damping coefficients c_1 and c_2 for fastenings and c_3 for spring need to be introduced.

In this particular case, the whole system is subjected to the following vertical excitation E_y:

$$E_y = A\ sin\ \omega t, \tag{7.31}$$

and its derivatives are as follows:

$$\dot{E}_y = A\omega\ cos\ \omega t, \tag{7.32}$$

$$\ddot{E}_y = -A\omega^2\ sin\ \omega t. \tag{7.33}$$

Using the Lagrangian mechanics the equations of motion will be derived. The generalised coordinates are φ_1 , φ_2 and l_1. Projecting the positions of the pendulum`s masses on the Cartesian coordinate system, shown in figure 23, we obtain:

$$r_{x1} = l_1 \sin\varphi_1, \tag{7.34}$$

$$r_{x2} = l_1 sin\varphi_1 + l_2 sin\varphi_2, \tag{7.35}$$

$$r_{y1} = l_1 \cos\varphi_1 - E_y, \tag{7.36}$$

$$r_{y2} = l_1 cos\varphi_1 - E_y + l_2 cos\varphi_2. \tag{7.37}$$

By integrating and summing (7.34) and (7.36), as well as (7.35) and (7.37), we obtain equations of velocities:

$$v_1 = (\dot{l_1}^2 - 2\dot{l_1}cos\varphi_1\dot{E_y} + {l_1}^2\dot{\varphi_1}^2 + 2l_1sin\varphi_1\dot{\varphi_1}\dot{E_y} + \dot{E_y}^2)^{\frac{1}{2}},$$

(7.38)

$$v_2 = (\,2l_1sin\varphi_1\dot{\varphi_1}\dot{E_y} + 2l_1\dot{\varphi_1}l_2\dot{\varphi_2}\cos(\varphi_1 - \varphi_2) - 2\dot{l_1}cos\varphi_1\dot{E_y} + \dot{E_y}^2 + {l_1}^2\dot{\varphi_1}^2 + \dot{l_1}^2 + 2l_2sin\varphi_2\dot{\varphi_2}\dot{E_y} + 2\dot{l_1}l_2\dot{\varphi_2}\sin(\varphi_1 - \varphi_2) + \dot{\varphi_2}^2{l_2}^2\,)^{\frac{1}{2}},$$

(7.39)

According to the definition 5(see chapter 2), the total kinetic energy of the system is given by (2.5). Substituting squares of (7.38) and (7.39) into (2.5), the total kinetic energy of the system is received:

$$\begin{aligned} T = \frac{1}{2}m_1\left(\dot{l_1}^2 - 2\dot{l_1}cos\varphi_1\dot{E_y} + {l_1}^2\dot{\varphi_1}^2 + 2l_1sin\varphi_1\dot{\varphi_1}\dot{E_y} + \dot{E_y}^2\right) \\ + \frac{1}{2}m_2\left(2l_1sin\varphi_1\dot{\varphi_1}\dot{E_y} + 2l_1\dot{\varphi_1}l_2\dot{\varphi_2}\cos(\varphi_1 - \varphi_2) - 2\dot{l_1}cos\varphi_1\dot{E_y}\right. \\ \left. + \dot{E_y}^2 + {l_1}^2\dot{\varphi_1}^2 + \dot{l_1}^2 + 2l_2sin\varphi_2\dot{\varphi_2}\dot{E_y} + 2\dot{l_1}l_2\dot{\varphi_2}\sin(\varphi_1 - \varphi_2)\right. \\ \left. + \dot{\varphi_2}^2{l_2}^2\right), \end{aligned}$$

(7.40)

whereas, its potential energy (on the basis of definition 6), for the special case of double pendulum, takes the following form:

$$V = m_1gl_1(1 - cos\varphi_1) + m_2g\big(l_1(1 - cos\varphi_1) + l_2(1 - cos\varphi_2)\big) + \frac{1}{2}k_1(l_1 - l_I)^2.$$

(7.41)

In order to calculate equations of motion, function of dissipation have to be also taken into consideration. For the special case, it takes the following form:

$$D = \frac{1}{2}c_1\dot{\varphi_1}^2 + \frac{1}{2}c_2(\dot{\varphi_2} - \dot{\varphi_1})^2 + \frac{1}{2}c_3\dot{l_1}^2.$$

(7.42)

Having calculated (7.40), (7.41) and (7.42) and substituting their adequate derivatives to Lagrange`s equations of the 2nd kind (see chapter 2, 2.14), we receive 3 equations of motion for the system given in fig. 23; 1 equation for each degree of freedom. They are as follows:

$$\ddot{\varphi}_1(m_1+m_2){l_1}^2 + \ddot{\varphi}_2 m_2 l_1 l_2 \cos(\varphi_1-\varphi_2) + 2\dot{\varphi}_1 \dot{l}_1 l_1 (m_1+m_2) + {\dot{\varphi}_2}^2 m_2 l_1 l_2 \sin(\varphi_1-\varphi_2) + (m_1+m_2)\left(g+\ddot{E}_y\right) sin\varphi_1 l_1 + c_1\dot{\varphi}_1 + c_2(\dot{\varphi}_1-\dot{\varphi}_2) = 0, \tag{7.43}$$

$$\ddot{\varphi}_1 m_2 l_1 l_2 \cos(\varphi_1-\varphi_2) + \ddot{\varphi}_2 m_2 {l_2}^2 + \ddot{l}_1 m_2 l_2 \sin(\varphi_1-\varphi_2) + 2\dot{\varphi}_1 \dot{l}_1 m_2 l_2 \cos(\varphi_1-\varphi_2) - {\dot{\varphi}_1}^2 m_2 l_1 l_2 \sin(\varphi_1-\varphi_2) + m_2 l_2 sin\varphi_2\left(g+\ddot{E}_y\right) + c_2(\dot{\varphi}_2-\dot{\varphi}_1) = 0, \tag{7.44}$$

$$\ddot{\varphi}_2 m_2 l_2 \sin(\varphi_1-\varphi_2) + \ddot{l}_1(m_1+m_2) - {\dot{\varphi}_2}^2 m_2 l_2 \cos(\varphi_1-\varphi_2) - \dot{\varphi}_1^2 l_1 (m_1+m_2) - (m_1+m_2)\cos\varphi_1\left(\ddot{E}_y+g\right) + (m_1+m_2)g + k_1(l_1-l_l) + c_3\dot{l}_1 = 0. \tag{7.45}$$

Recalling the rearranged general matrix representation of the equations of motion:

$$M\ddot{q} = R. \tag{7.23}$$

Putting equations (7.43), (7.44) and (7.45) into (7.23), we obtain 3 dimensional system of equations of motion in matrix form, presented below:

$$\mathrm{M} = \begin{bmatrix} (m_1 + m_2){l_1}^2 & m_2 l_1 l_2 \cos(\varphi_1 - \varphi_2) & 0 \\ m_2 l_1 l_2 \cos(\varphi_1 - \varphi_2) & \mathrm{m_2 l_2^2} & \mathrm{m_2 l_2 \sin(\varphi_1 - \varphi_2)} \\ 0 & \mathrm{m_2 l_2 sin(\varphi_1 - \varphi_2)} & \mathrm{(m_1 + m_2)} \end{bmatrix}, \tag{7.46}$$

$$\ddot{q} = \begin{pmatrix} \ddot{\varphi}_1 \\ \ddot{\varphi}_2 \\ \ddot{l}_1 \end{pmatrix}, \tag{7.47}$$

$$R = \begin{bmatrix} 2\dot{\varphi}_1 \dot{l}_1 l_1 (m_1 + m_2) + {\dot{\varphi}_2}^2 m_2 l_1 l_2 \sin(\varphi_1 - \varphi_2) + (m_1 + m_2)\left(g + \ddot{E}_y\right) sin\varphi_1 l_1 + c_1 \dot{\varphi}_1 + c_2(\dot{\varphi}_1 - \dot{\varphi}_2) \\ 2\dot{\varphi}_1 \dot{l}_1 m_2 l_2 \cos(\varphi_1 - \varphi_2) - {\dot{\varphi}_1}^2 m_2 l_1 l_2 \sin(\varphi_1 - \varphi_2) + m_2 l_2 sin\varphi_2 \left(g + \ddot{E}_y\right) + c_2(\dot{\varphi}_2 - \dot{\varphi}_1) \\ -{\dot{\varphi}_2}^2 m_2 l_2 \cos(\varphi_1 - \varphi_2) - \dot{\varphi}_1^2 l_1 (m_1 + m_2) - (m_1 + m_2)\cos\varphi_1 \left(\ddot{E}_y + g\right) + (m_1 + m_2) g + k_1(l_1 - l_l) + c_3 \dot{l}_1 \end{bmatrix}. \tag{7.48}$$

7.3 Comparison of the cases

While system presented in subchapter 7.2 is simplified version of the double pendulum from section 7.1, it is relatively simple to verify, whether the examined system is derived properly, basing on the general case. Since in the special case there are only 3 degrees of freedom, unlike 4 DOFs from the general case, then it is reduced to 3 equations of motion and as the consequence size of the mass matrix M is 3×3 and of rest matrix R is 3×1.

Comparing both cases we notice that matrix (7.46) is inscribed into (7.26) i.e. it occupies its top-left position and their particular elements correspond to each other. As for the generalised coordinates, in the special case there are only 3 of them due to fewer degrees of freedom, see (7.27) and (7.47). Furthermore, removing components with $\dot{l}_2$ and setting the parameters from the rest matrix R (7.28) like k_2, c_4 and horizontal component of excitation E_x to zero we obtain the rest matrix R related to the special case (7.48).

The above elaboration proves, that system is derived correctly and properly.

8. Numerical analysis

This chapter is devoted to the investigation and analysis of the behaviour of the double pendulum system, presented in chapter 7.2, which is the subject of this paper. The research utilises the specially written software for the mathematical computations concerning this task. Additionally graphical program was used in order to gather data and create diagrams.

8.1 Research input data

There are a few steps necessary to understand the motion of the given system. The most reliable tool in analysis are bifurcation diagrams, which make it possible to verify how a negligible increment or decrement of a chosen parameter influence the dynamics of the whole system. Moreover, as the additional chaos detection instrument Poincaré maps were used. Finally, phase portraits and time diagrams were created.

The numerical investigation of the double pendulum with parametric, vertical excitation system, was performed for the following set of parameters:

$m_1 = 2$ kg,

$m_2 = 3$ kg,

$k = 2500$ N/m,

$l_1 = 0.6$ m,

$l_2 = 0.6$ m,

$c_1 = 0.017\, m_1 \sqrt{g\, {l_1}^3}$ $\frac{kg\, m^2}{s}$,

$c_2 = 0.011\, m_2 \sqrt{g\, {l_2}^3}$ $\frac{kg\, m^2}{s}$,

$c_3 = 0.02 \sqrt{k_1 (m_1 + m_2)}$ $\frac{kg}{s}$,

$Amplitude = 0.25$ m.

(set 8.1)

and the set of the initial conditions:

$\varphi_1 = 0.5,$

$\varphi_2 = 0.2,$

$l_1 = l_I,$

$\dot{\varphi_1} = 0.0,$

$\dot{\varphi_2} = 0.0,$

$\dot{l_1} = 0.0.$

(set 8.2)

The research is performed when system indicates stable behaviour – i.e proper vibrations of the system disappear and it is subjected to the forced vibrations only, that is a reason, why the specific number of periods is omitted and data collection is started at the particular step (there are 200 stabilising periods followed by 100 periods recorded).

8.2 Analysis of the excitation frequency influence

At first, the influence of excitation frequency on the behaviour of the double pendulum system with parametric, vertical excitation is investigated.

8.2.1 Bifurcation diagrams for excitation frequency

There are the bifurcation diagrams, for data given in set 8.1 and initial conditions in set 8.2, with excitation frequency taken as the bifurcation parameter, presented below. For convenience, the same variable for forward and backward direction of investigation were put on the same page.

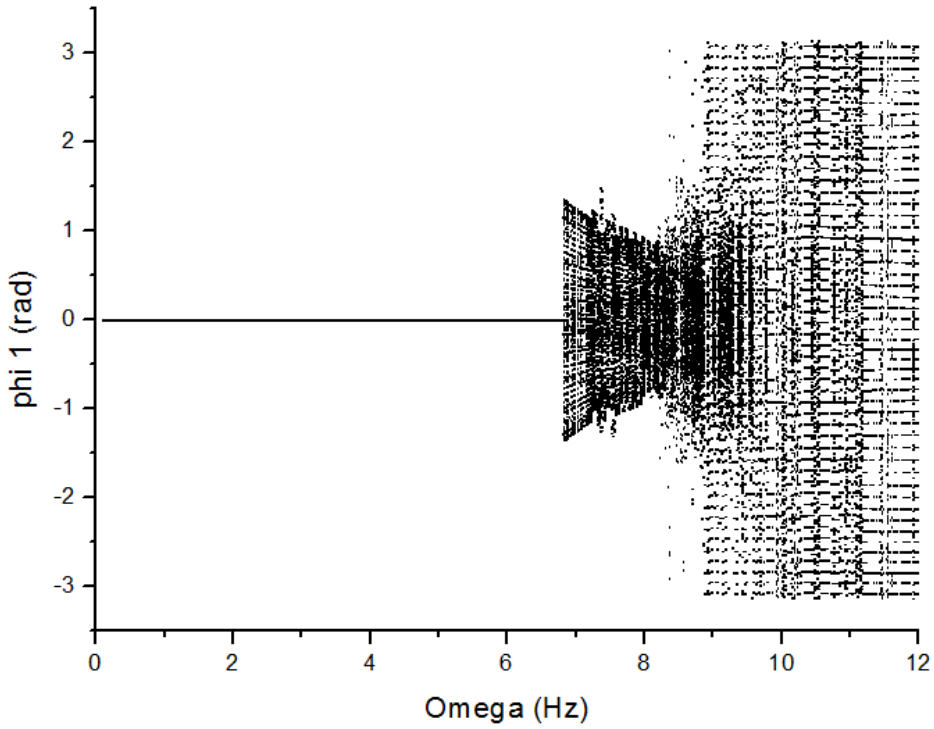

Fig. 24 Forward bifurcation diagram for angle φ_1 and excitation frequency ω.

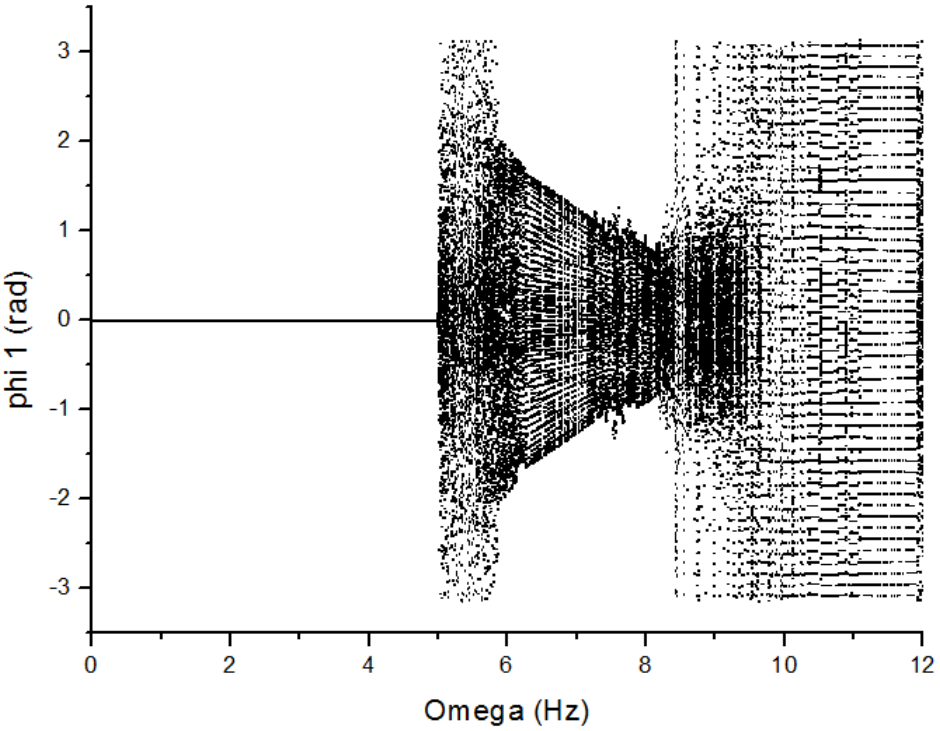

Fig. 25 Backward bifurcation diagram for angle φ_1 and excitation frequency ω.

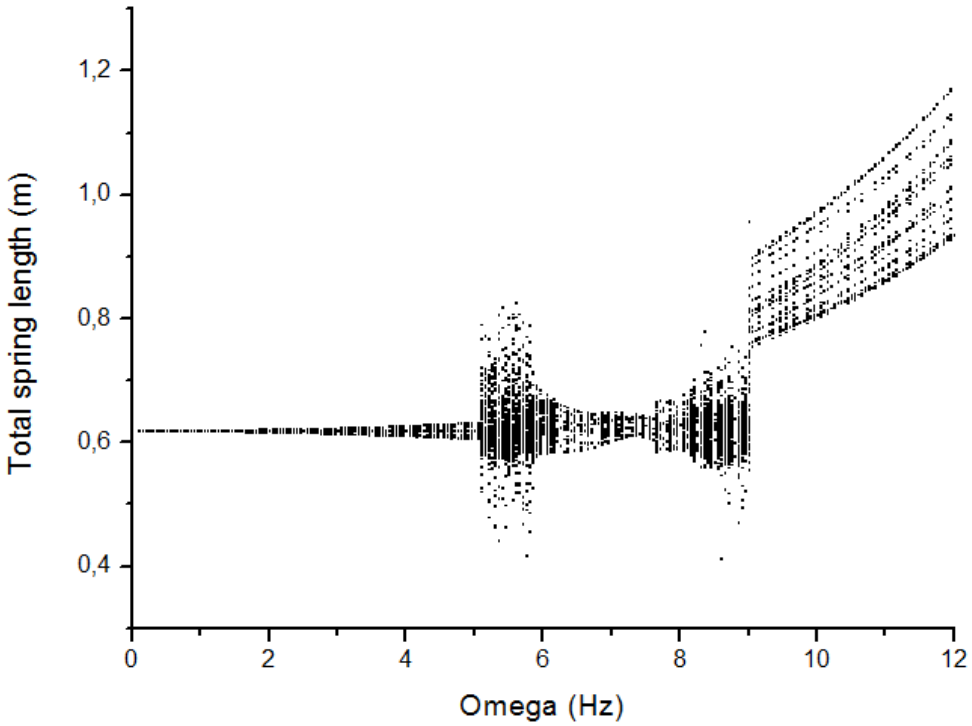

Fig. 26 Forward bifurcation diagram for total spring length l_1 and excitation frequency ω.

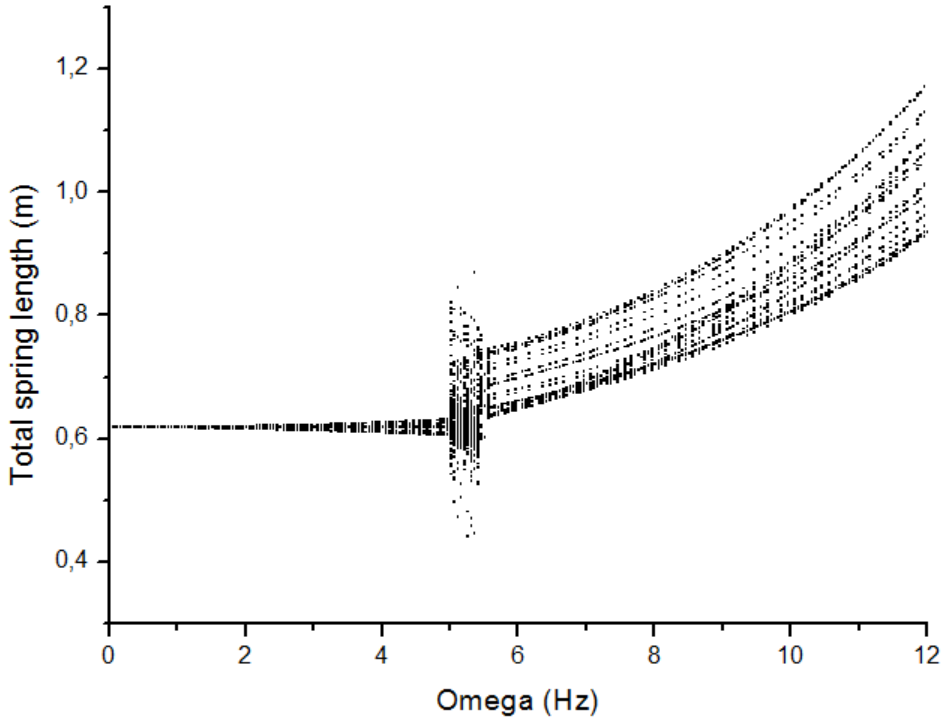

Fig. 27 Backward bifurcation diagram for total spring length l_1 and excitation frequency ω.

The bifurcation diagrams were created in two directions of the parameter change. At first, simulation was started forwards, then, after reaching the limit, and applying the end conditions as the initial conditions, simulation was restarted backwards. It occurred, that solutions vary, indicating coexistence of attractors, what can be noticed in bifurcation diagrams, presented in figures 27 to 30. Generally, areas of the altered behaviour of the system differs significantly for forward and backward bifurcations.

The bifurcation diagrams presented in figure 27 concern change of declination angle φ_1 with respect to the excitation frequency ω in range of (0.01 to 12) Hz. We observe periodic motion until $\omega = 5.1$ Hz, where saddle-node bifurcation occurs. Due to the loss of the stability of the system, motion changes into chaotic one. Such a situation is kept until $\omega = 5.9$ Hz, starting at that point, until $\omega = 9.0$ Hz, system is in a temporary section. Then, the attractor change proceeds and as the consequence, there is a rapid change of the behaviour of the system, which is now multiperiodic, until the end of the measuring range. In case of diagrams 28 and 30, at the end of the phase of chaotic motion, we observe inversed period doubling for $\omega = 5.5$ Hz, followed by the multiperiodic motion.

An interesting phenomena occur for bifurcations presenting total spring length depending on excitation frequency. We observe, that after some critical value of ω, spring begins to elongate rapidly, while subjected to the periodic motion. The possible explanation for that are rotations of the end pendulum. As the consequence of the action of positional force, spring`s length is increasing.

8.2.2 Poincaré maps for excitation frequency

The Poincaré maps presented below, proves the assumption for chaotic motion for excitation frequency $\omega = 5.5\ Hz$, points are scattered and no pattern can be found. Whereas, study of case for $\omega = 8.2\ Hz$, reveals that motion for that value of excitation frequency is multiperiodic. Additionally, there are Poincaré maps for spring for every behaviour of the system, described above, i.e. for $\omega = 1\ Hz,\ 7\ Hz,\ 10.5\ Hz$. These diagrams reveal that motion for those values of excitation frequency are either periodic or multiperiodic.

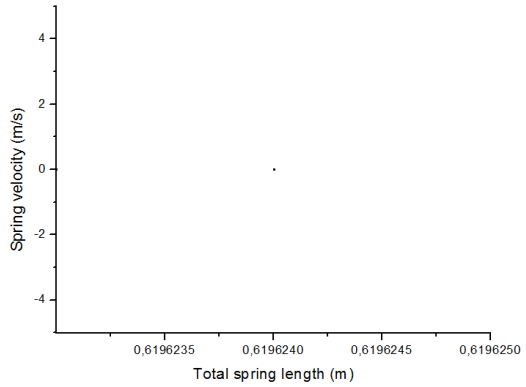

Fig. 28 Poincaré map for excitation frequency $\omega = 1$ Hz.

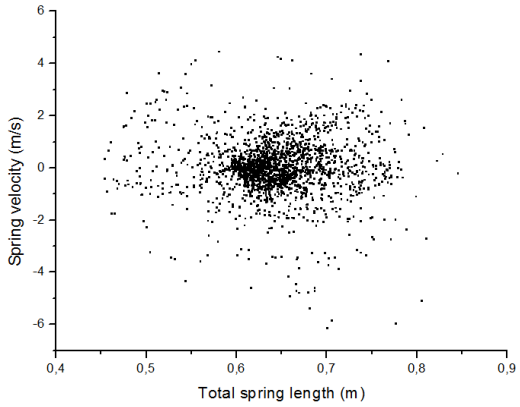

Fig. 29 Poincaré map for excitation frequency $\omega = 5.5$ Hz.

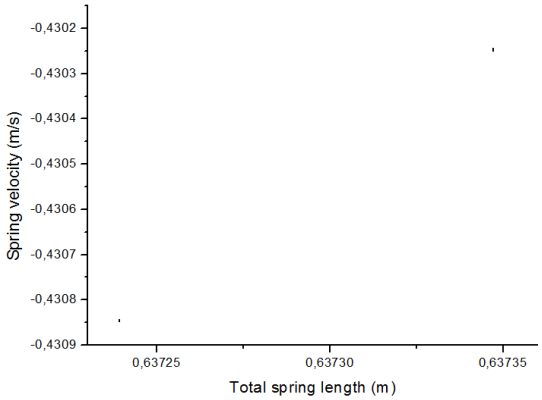

Fig. 30 Poincaré map for excitation frequency $\omega = 7$ Hz.

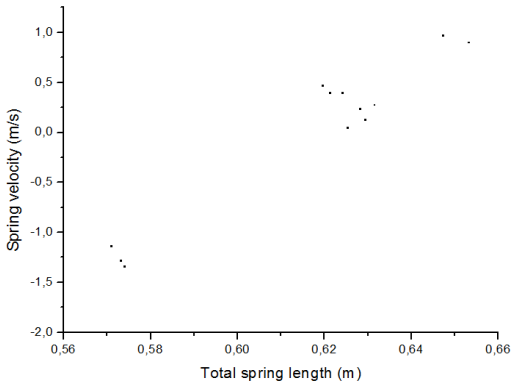

Fig. 31 Poincaré map for excitation frequency $\omega = 8.2$ Hz.

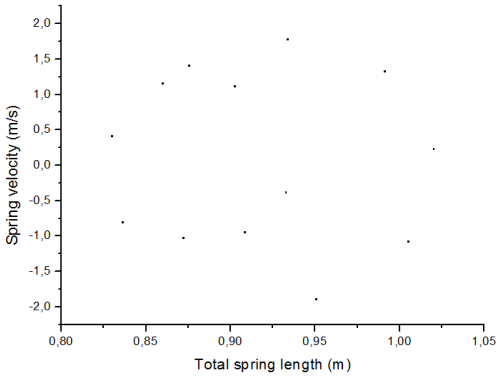

Fig. 32 Poincaré map for excitation frequency $\omega = 10.5$ Hz.

8.2.3 Phase portraits for excitation frequency

There are phase portraits for every investigated frequency resented below. While we are only interested in behaviour mapping, only phase portraits concerning spring are shown. All diagrams were created for the same time interval, when the system was stable.

One can see, that every diagram, except the one for excitation frequency $\omega = 5.5\,Hz$, show the periodic or multiperiodic motion. The distinguished case prove chaotic motion.

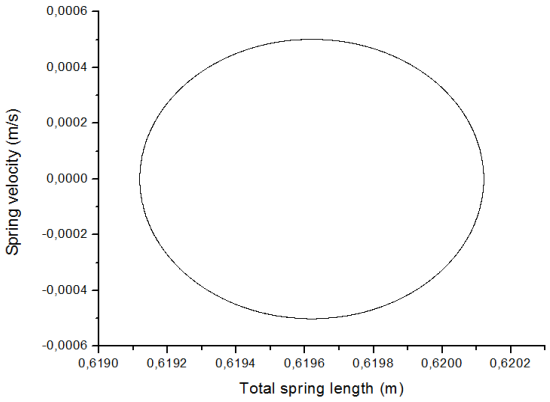

Fig. 33 Phase portrait for excitation frequency $\omega = 1$ Hz.

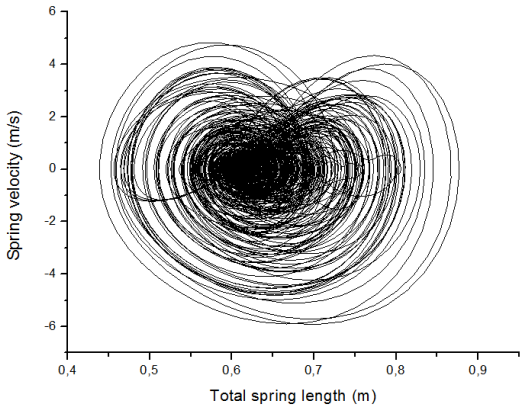

Fig. 34 Phase portrait for excitation frequency $\omega = 5.5$ Hz.

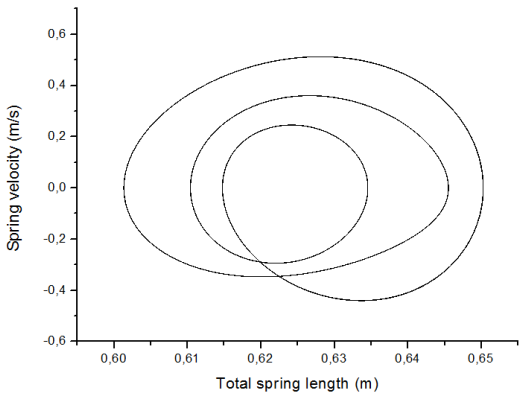

Fig. 36 Phase portrait for excitation frequency $\omega = 7$ Hz.

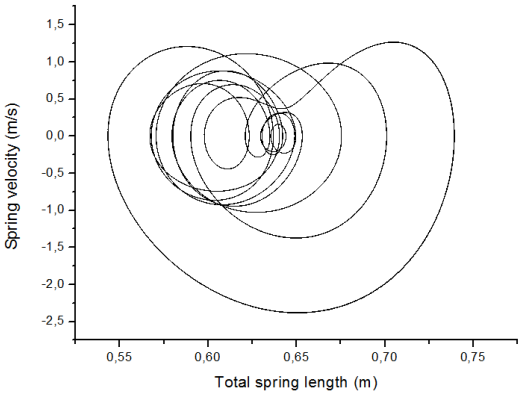

Fig. 35 Phase portrait for excitation frequency $\omega = 8.2$ Hz.

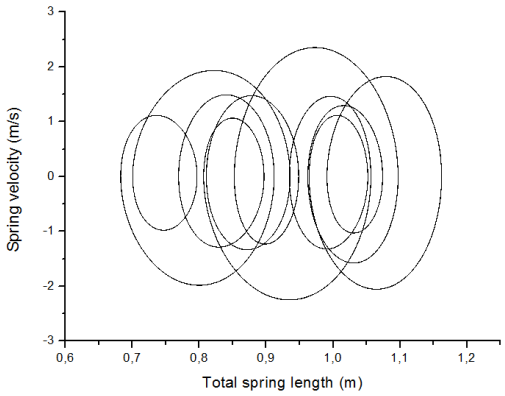

Fig. 37 Phase portrait for excitation frequency $\omega = 10.5$ Hz.

8.2.4 Time diagrams

The simplest way to visualize the motion of the body is to create diagrams showing dependency of a chosen parameter with respect to the time. There are the declination angles φ_1, φ_2 and total spring length $l_1$versus time diagrams. They were created for set 8.1 and set 8.2 with excitation frequency $\omega = 5.5\ Hz$. One can see, that there are no distinctive similarities or patterns in the whole analysed interval, and thus the system indicates chaotic behaviour.

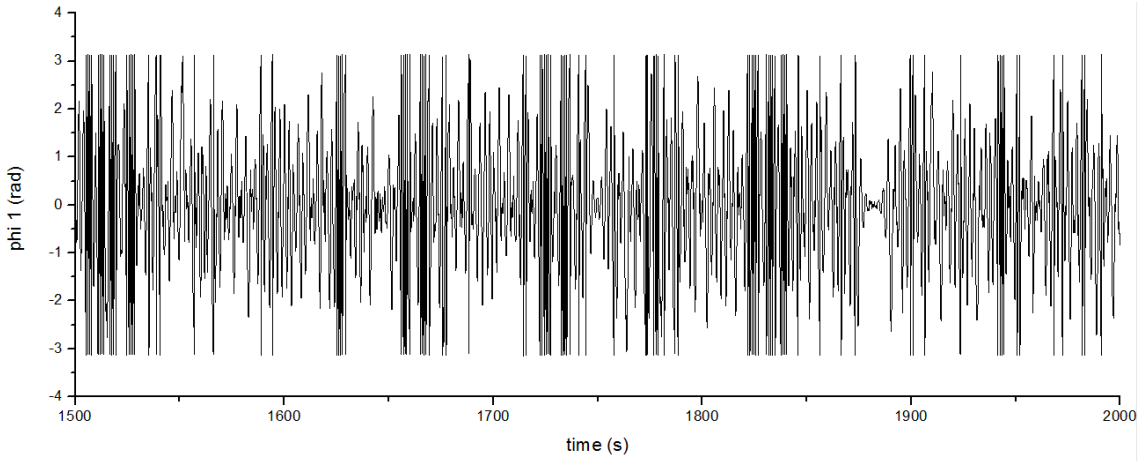

Fig. 38 Angle φ_1 change vs time for excitation frequency $\omega = 5.5\ Hz$.

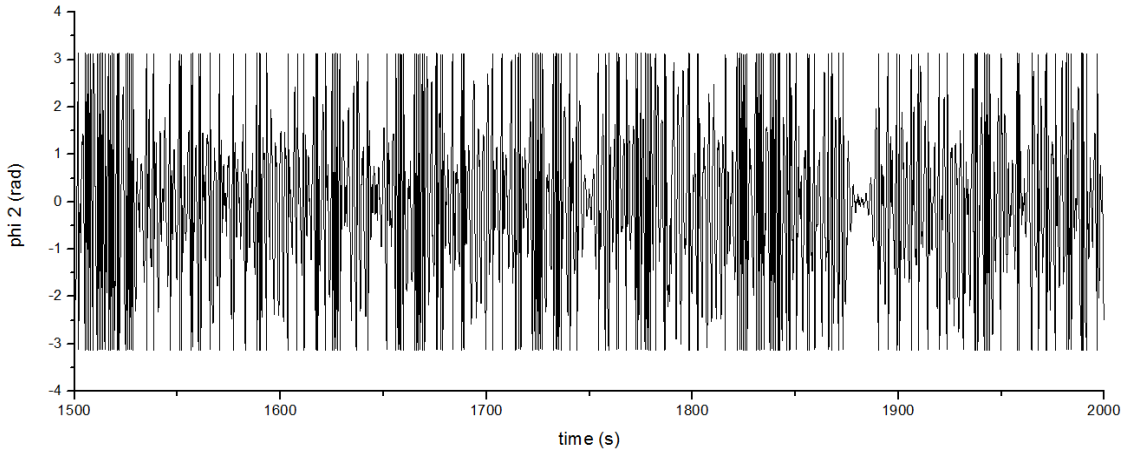

Fig. 39 Angle φ_2 change vs time for excitation frequency $\omega = 5.5\ Hz$.

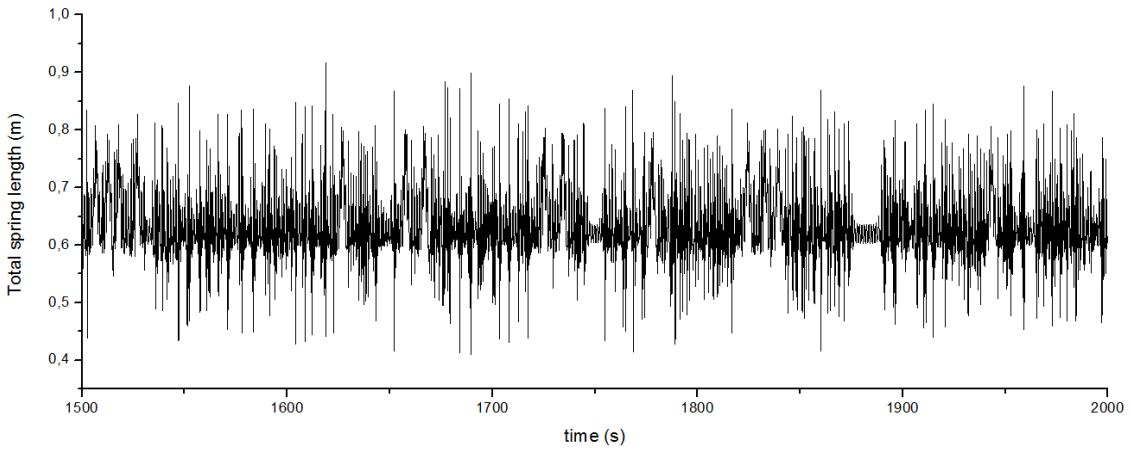

Fig. 40 Total spring length l_1 change vs time for excitation frequency $\omega = 5.5\ Hz$.

8.3 Analysis of the stiffness coefficient influence

In this subchapter, the influence of the stiffness coefficient of the spring on the behaviour of the double pendulum system with parametric, vertical excitation is investigated. The assumed excitation frequency ω is constant for all considered cases and equal to 8.5 Hz.

8.3.1 Bifurcation diagrams for stiffness coefficient

There are the bifurcation diagrams, for data given in set 8.1 and initial conditions in set 8.2, with stiffness coefficient taken as the bifurcation parameter, presented below. The excitation frequency ω is set to 8.5 Hz.

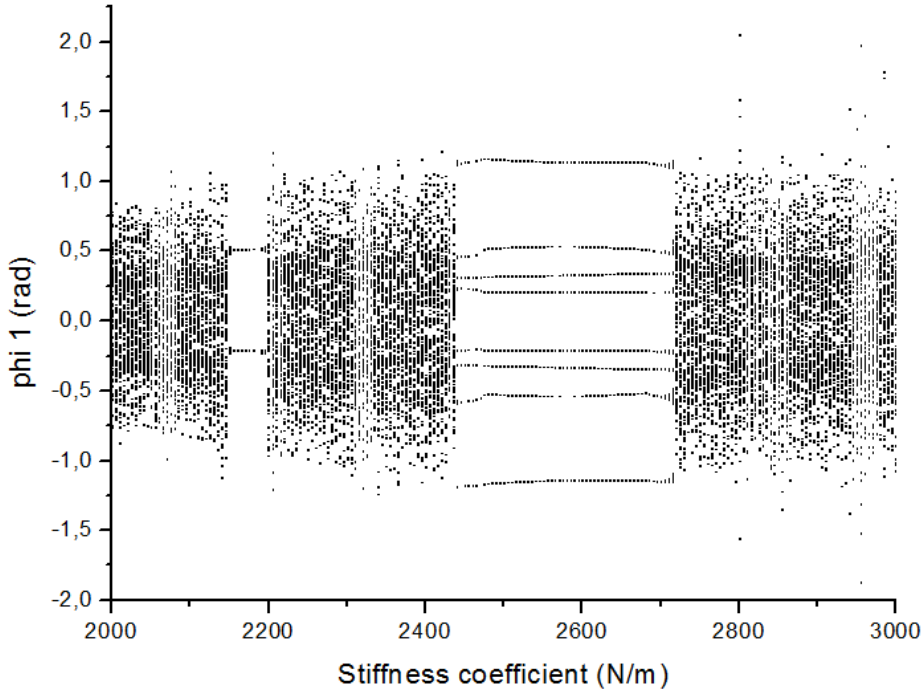

Fig. 41 Forward bifurcation diagram for angle φ_1 and stiffness coefficient k.

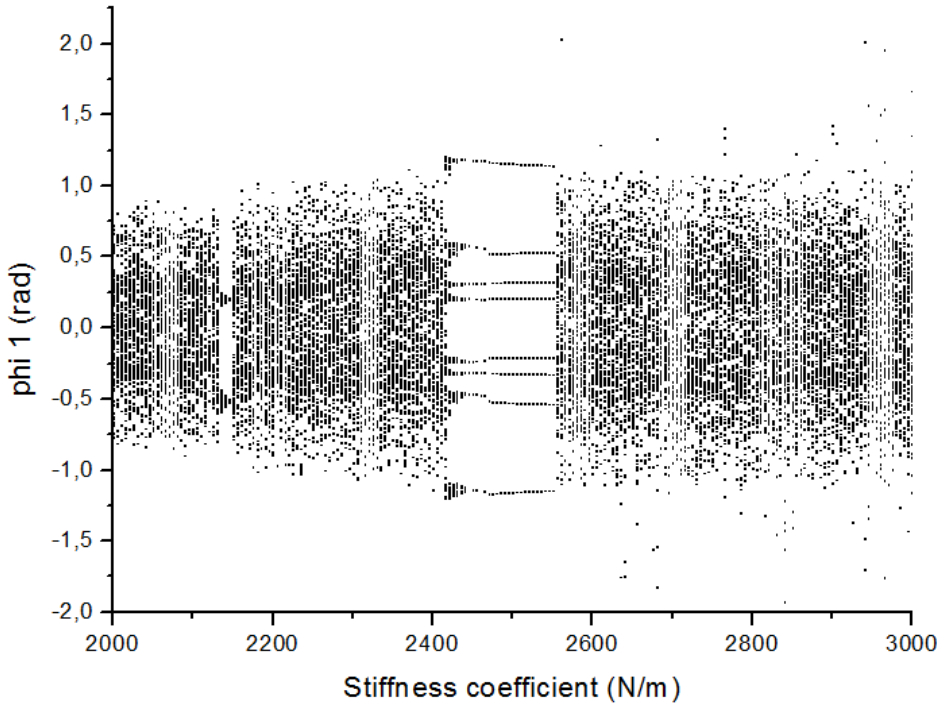

Fig. 42 Backward bifurcation diagram for angle φ_1 and stiffness coefficient k.

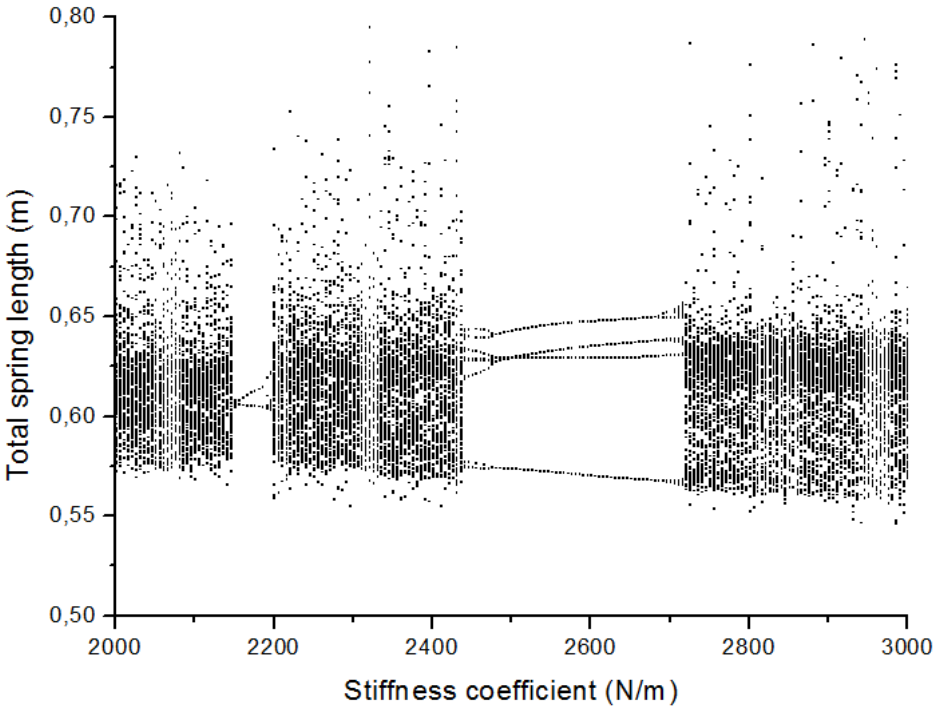

Fig. 43 Forward bifurcation diagram for total spring length l_1 and stiffness coefficient k.

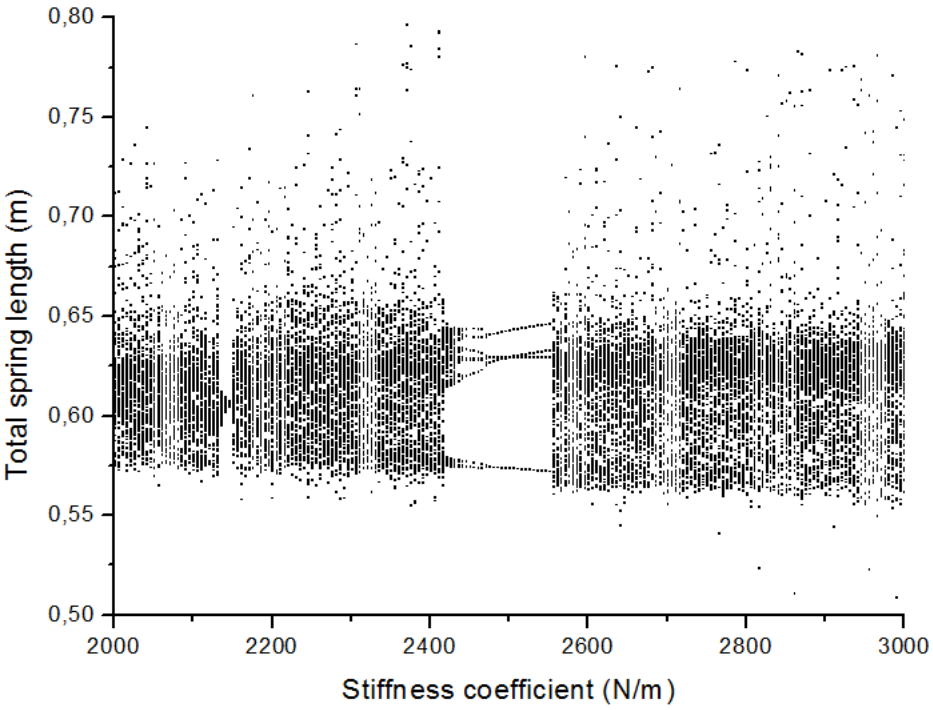

Fig. 44 Backward bifurcation diagram for total spring length l_1 and stiffness coefficient k.

For the better insight into the systems behaviour, there is the magnification of the one of the most interesting areas for stiffness coefficient k ranging from 2130 to 2180.

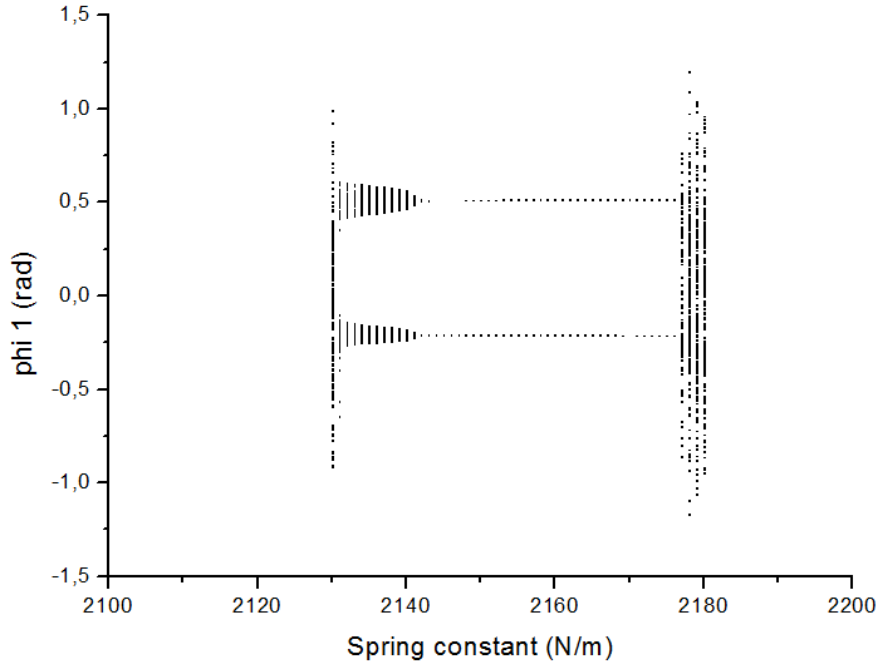

Fig. 45 Magnified backward bifurcation diagram for angle φ_1 versus stiffness coefficient k.

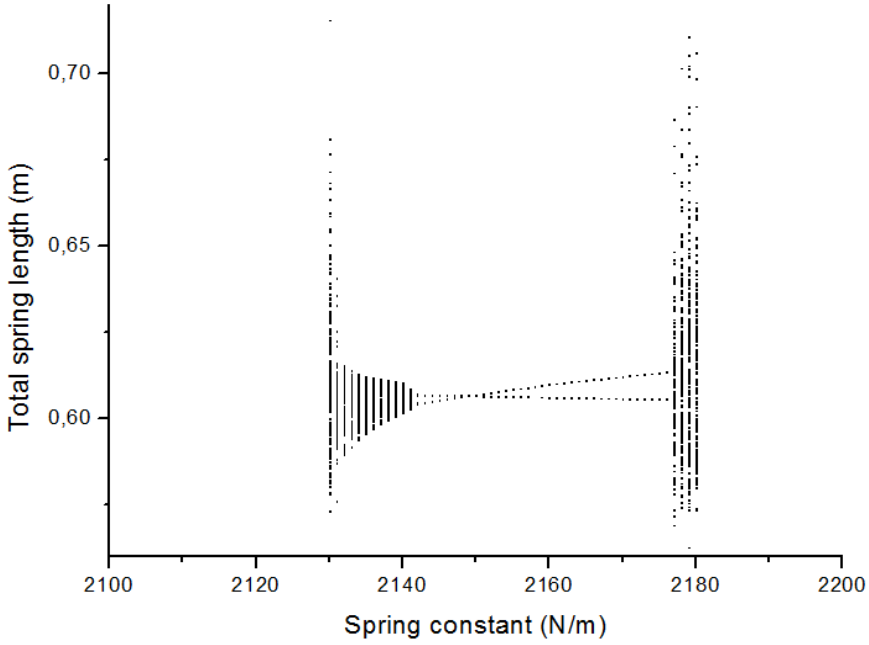

Fig. 46 Magnified backward bifurcation diagram for total spring length l_1 versus stiffness coefficient k.

The other zone of more accurate calculations is performed for the second window occurring on bifurcation diagrams, ranging from (2470 to 2710) N/m. For convenience and diagram clearance, only 3 top branches are shown.

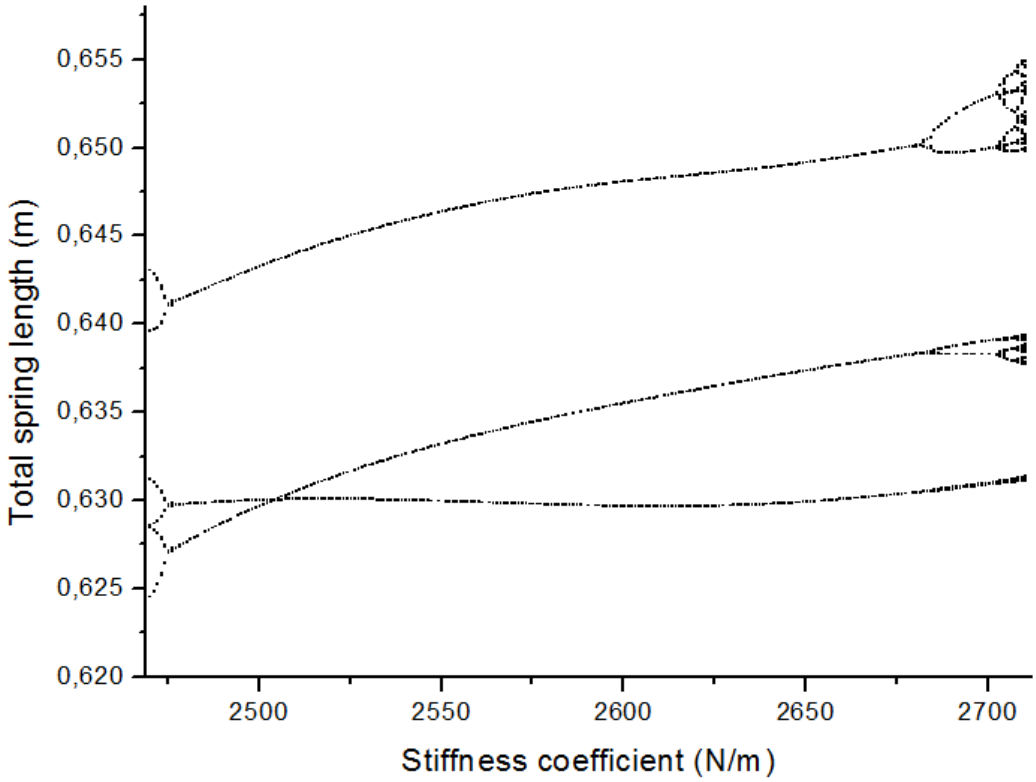

Fig. 47 Magnified forward bifurcation diagram for total spring length l_1 versus stiffness coefficient k.

The bifurcation diagrams presented in section 8.3.2 concern change of declination angle φ_1 and total spring length l_1 with respect to the stiffness coefficient k in range of (2000 to 3000) N/m. We observe irregular motion in almost whole investigated range. We may distinguish 2 windows with periodic motion, for $k = 2130$ to 2180 and similarly, for $k = 2470$ to 2710 for forward analysis, and for k = 2470 to 2550 for backward analysis. The closer investigation of the 1 window, suggests that we deal with the secondary Hopf bifurcation (Neimark bifurcation) in that range, i.e. transition from periodic to quasiperiodic motion is seen. Whereas, in the second window, the transition from chaotic motion to regular one takes place via sequences of period doubling bifurcation. Similarly, for stiffness coefficient around $k = 2700\ N/m$, one may observe period doubling phenomena as the route to chaos.

The bifurcation diagrams were, again, created in two directions of the parameter change. At first, simulation was started forwards, then, after reaching

the limit, and applying the end conditions as the initial conditions, simulation was restarted backward. It occurred, that solutions slightly vary, what is especially visible in *windows.* indicating coexistence of attractors. Generally, forward and backward bifurcations are very similar, but for the backward direction, we observe that the switch of the solution occurs later (starting from $k = 3000$, there is a longer period of probable chaotic motion, until $k = 2550$).

8.3.2 Poincaré maps for stiffness coefficient

The Poincaré maps presented below, prove the assumption for chaotic motion in the mentioned areas, points are scattered and no pattern can be found. Whereas, for periodic motion, adequate diagrams also can be seen. Moreover, for the case $k = 2135\ N/m$, quasiperiodic motion is revealed.

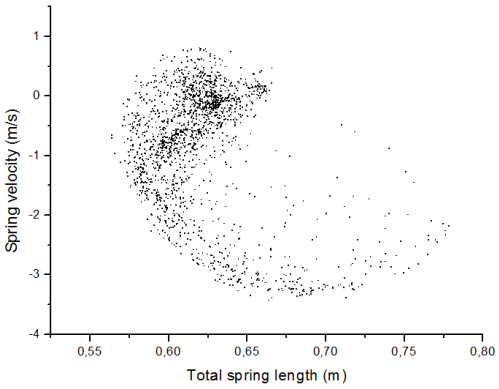

Fig. 48 Poincaré map for stiffness coefficient k = 2100 N/m.

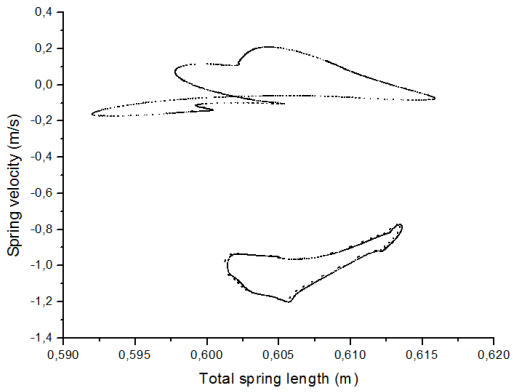

Fig. 49 Poincaré map for stiffness coefficient k = 2135 N/m.

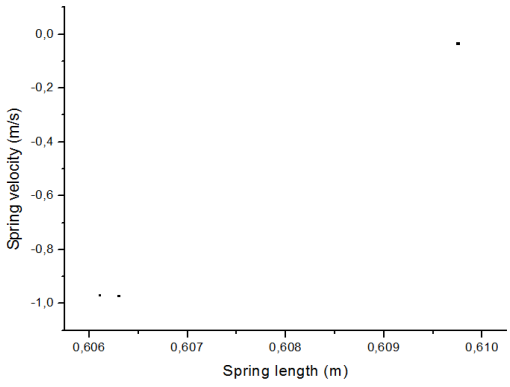

Fig. 50 Poincaré map for stiffness coefficient k = 2160 N/m.

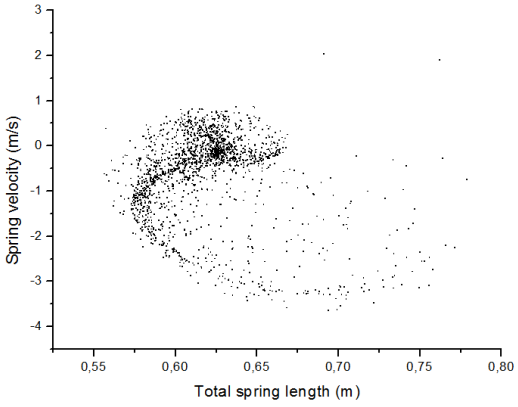

Fig. 51 Poincaré map for stiffness coefficient k = 2300 N/m.

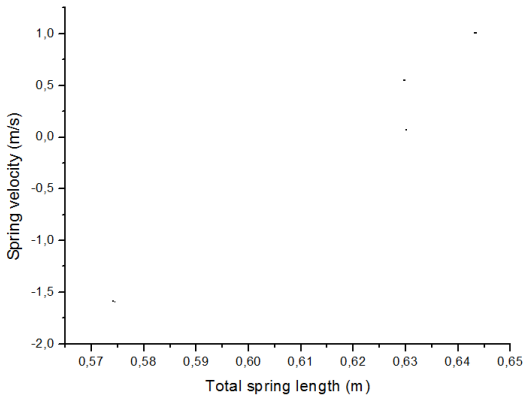

Fig. 52 Poincaré map for stiffness coefficient k = 2500 N/m.

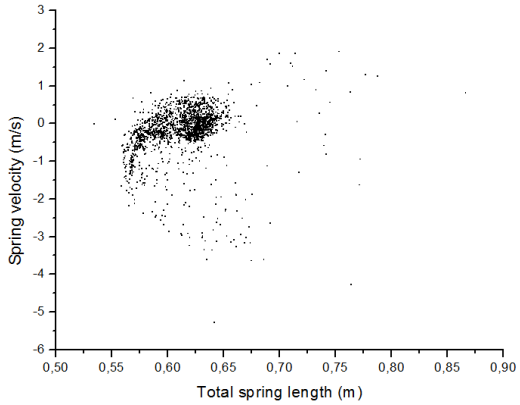

Fig. 53 Poincaré map for stiffness coefficient k = 2900 N/m.

8.3.3 Phase portraits for stiffness coefficient

The phase portraits for every investigated stiffness coefficient are presented below. There are only phase portraits concerning spring, while we are only interested in the behaviour mapping. All diagrams were created for the same time interval, when the system indicated stable behaviour. All possible solutions are again visible, chaotic motion, quasiperiodic and periodic ones.

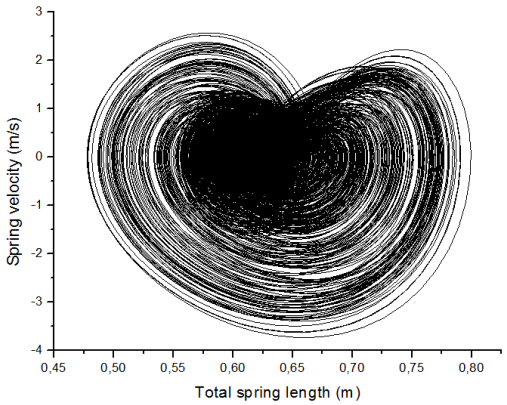

Fig. 54 Phase portrait for stiffness coefficient k = 2100 N/m..

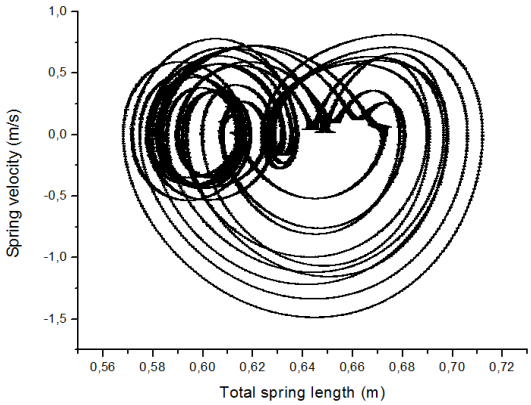

Fig. 55 Phase portrait for stiffness coefficient k = 2135 N/m..

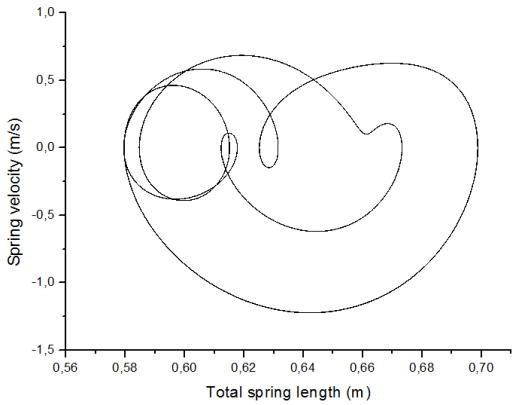

Fig. 56 Phase portrait for stiffness coefficient k = 2160 N/m..

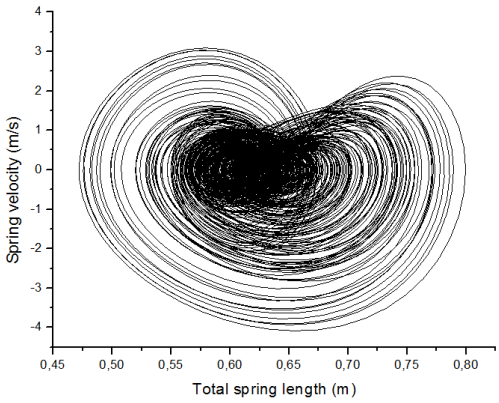

Fig. 57 Phase portrait for stiffness coefficient k = 2300 N/m..

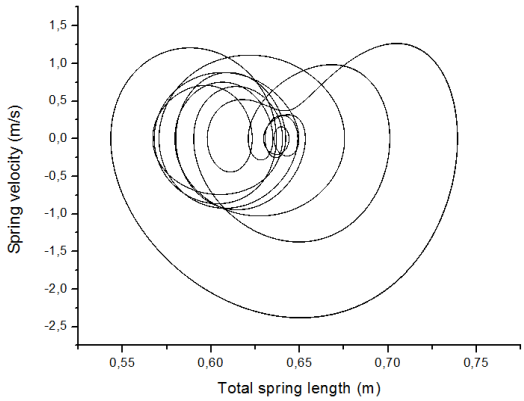

Fig. 58 Phase portrait for stiffness coefficient k = 2500 N/m..

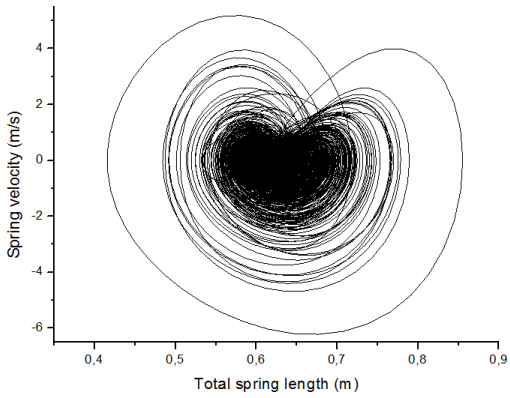

Fig. 59 Phase portrait for stiffness coefficient k = 2900 N/m..

8.3.4 Time diagrams

The simplest way to visualize the motion of the body is to create diagrams showing dependency of a chosen parameter with respect to the time. There are the declination angles φ_1, φ_2 and total spring length $l_1$versus time diagrams. Diagrams were created for set 8.1 and set 8.2 with stiffness coefficient $k = 2300\ N/m$. One can see, that there are no distinctive similarities or patterns in the whole analysed interval, and thus the system indicates chaotic behaviour.

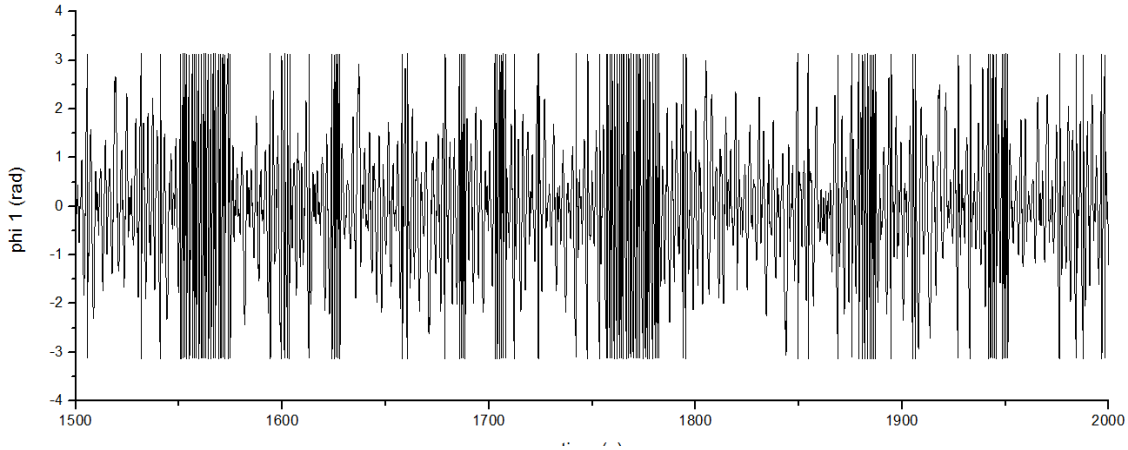

Fig. 60 Angle φ_1 change vs time for excitation frequency $\omega = 8.5\ Hz$ and stiffness coefficient $k = 2300\ N/m$.

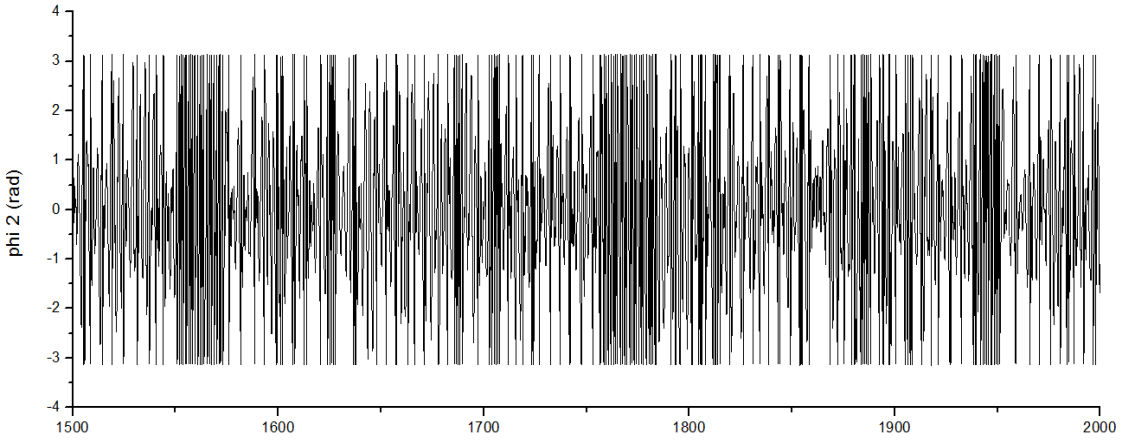

Fig. 61 Angle φ_2 change vs time for excitation frequency $\omega = 8.5\ Hz$ and stiffness coefficient $k = 2300\ N/m$.

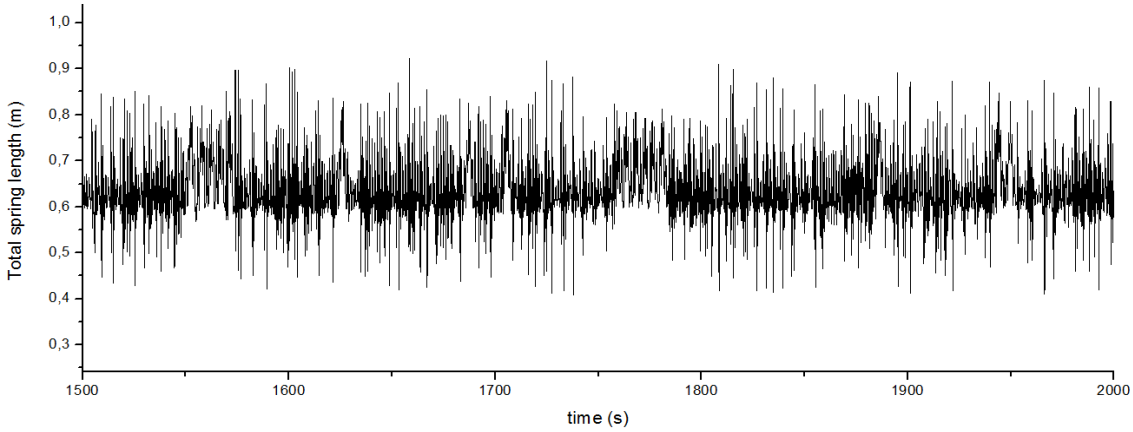

Fig. 62 Total spring length l_1 change vs time for excitation frequency $\omega = 8.5\ Hz$ and stiffness coefficient $k = 2300\ N/m$.

9. Conclusions

The numerical analysis performed for the double pendulum parametrically excited allow us to draw number of conclusions. First of all, the characteristic behaviour indicates, that the investigated system shows greatly nonlinear dynamics. There exist intervals of control parameters, depending on which, either periodic (including multiperiodic) motion or chaotic motion of the system is observed. Additionally, quasiperiodic motion was found. Furthermore, as proved, in some cases there is a possibility of coexistence of attractors, having influence on the motion. During the research, rapid change of motion from periodic to chaotic was shown according to saddle-node bifurcation for excitation frequency. As in case of the stiffness coefficient, taken as the bifurcation parameter, route to chaos was obtained via period doubling and Hopf bifurcations.

To conclude, the performed investigation indicates sensitivity of the examined system to control parameters, resulting in sudden changes of the system`s behaviour. It means, that rapid alteration of the behaviour of the system might be noticed, as the response to its control parameters change.

In technical literature, chaotic system is frequently understood as the system, whose numerical simulations suggest existence of complex dynamics. However, it is hardly ever assumed, that complicated attractor is in reality, the periodic trajectory of extremely large period; or we deal with quasiperiodic motion.

References

[1] Baker Gregory L., Blackburn James A., *The pendulum A case study in physics*, Oxford University Press, New York, 2005.

[2] Kapitaniak Tomasz, Wojewoda Jerzy, *Bifurkacje i Chaos*, Wydawnictwo Politechniki Łódzkiej, Łódź, 1995.

[3] Kapitaniak Tomasz, *Chaotic oscillations In mechanical systems,* Manchester University Press, 1991.

[4] Kapitaniak Tomasz, *Wstęp do teorii drgań,* Wydawnictwo Politechniki Łódzkiej, Łódź, 2005.

[5] Niedoba Janina, Niedoba Wiesław, *Równania różniczkowe zwyczajne i cząstkowe*, Uczelniane Wydawnictwa Naukowo-Dydaktyczne, Kraków, 2001.

[6] Rubinowicz Wojciech, Królikowski Wojciech, *Mechanika teoretyczna,* Wydawnictwa Naukowe PWN, Warszawa, 1998.

[7] Taylor John R., *Classical Mechanics,* University Science Books, United States of America, 2005.

[8] Vinogradov Oleg, *Fundamentals of kinematics and dynamics of machines and mechanisms,* CRC Press LLC, United States of America, 2000.

[9] http://im0.p.lodz.pl/~bprzeradzki/uk-dyn.pdf

[10] http://mathworld.wolfram.com/PeriodicFunction.html

[11] Linda K. , Kowaluk M. , *Zobaczyć chaos…* , PowerPoint presentation, 2010